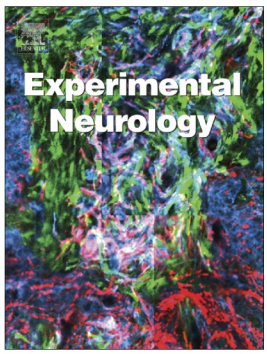

PTK2B/Pyk2 overexpression improves a mouse model of Alzheimer's disease

Albert Giralt, Benoît de Pins, Carmen Cifuentes-Díaz, Laura López-Molina, Amel Thamila Farah, Marion Tible, Vincent Deramecourt, Stefan Arold, Silvia Ginés, Jacques Hugon, Jean-Antoine Girault

PII: S0014-4886(18)30160-2
DOI: doi:10.1016/j.expneurol.2018.05.020
Reference: YEXNR 12765

To appear in: *Experimental Neurology*

Received date: 23 January 2018
Revised date: 14 May 2018
Accepted date: 23 May 2018

Please cite this article as: Albert Giralt, Benoît de Pins, Carmen Cifuentes-Díaz, Laura López-Molina, Amel Thamila Farah, Marion Tible, Vincent Deramecourt, Stefan Arold, Silvia Ginés, Jacques Hugon, Jean-Antoine Girault , PTK2B/Pyk2 overexpression improves a mouse model of Alzheimer's disease. The address for the corresponding author was captured as affiliation for all authors. Please check if appropriate. Yexnr(2017), doi:10.1016/j.expneurol.2018.05.020

PTK2B/Pyk2 overexpression improves a mouse model of Alzheimer's disease

Albert Giralt[1, 2, 3, 4, 5, 6], Benoît de Pins[1, 2, 3], Carmen Cifuentes-Díaz[1, 2, 3], Laura López-Molina[4, 5, 6], Amel Thamila Farah[1, 2, 3§], Marion Tible[7, 8], Vincent Deramecourt[9], Stefan Arold[10], Silvia Ginés[4, 5, 6], Jacques Hugon[7, 8], and Jean-Antoine Girault[1, 2, 3]*

[1] Inserm UMR-S 839, Paris, France

[2] *Sorbonne Université*, Science and Engineering Faculty, Paris, France

[3] *Institut du Fer a Moulin*, Paris, France.

[4] Departament de Biomedicina, Facultat de Medicina, Institut de Neurociències, Universitat de Barcelona, 08036 Barcelona, Spain

[5] Institut d'Investigacions Biomèdiques August Pi i Sunyer (IDIBAPS), 08036 Barcelona, Spain

[6] Centro de Investigacion Biomedica en Red Sobre Enfermedades Neurodegenerativas (CIBERNED), 28031 Madrid, Spain.

[7] Inserm UMR-S 942, Paris, France.

[8] Research Memory Center, Paris-Nord Ile-de-France, Saint-Louis-Lariboisière-Fernand Widal Hospital, Paris, France.

[9] Univ Lille, CHU Lille, INSERM U1172 "Alzheimer et Tauopathies", LabEx DISTALZ, 59000 Lille, France

[10] King Abdullah University of Science and Technology (KAUST), Center for Computational Bioscience Research (CBRC), Division of Biological and Environmental Sciences and Engineering (BESE), Thuwal, 23955-6900, Saudi Arabia.

§ Current address, *Centre de Neurosciences et Psychiatrie*, UMR-S894, Inserm and *Université Paris Descartes*, Paris, France

* Correspondence to: Dr J.-A. Girault
Institut du Fer a Moulin, Inserm and UPMC UMR-S839
Tel: + 33 1 45 87 61 52
E-mail: jean-antoine.girault@inserm.fr

E-Mail addresses:

Stefan Arold stefan.arold@kaust.edu.sa ; Carmen Cifuentes-Díaz carmen.diaz@inserm.fr ; Benoît de Pins benoit.de-pins@inserm.fr ; Vincent Deramecourt vincent.deramecourt@chru-lille.fr ; Silvia Gines silviagines@ub.edu ; Albert Giralt albertgiralt@ub.edu ; Jacques Hugon jacques.hugon@inserm.fr ; Laura López-Molina lauralopez-molina@ub.edu ; Amel Thamila Farah amelfarahth@gmail.com ; Marion Tible marion.tible@gmail.com

Abstract

Pyk2 is a Ca^{2+}-activated non-receptor tyrosine kinase enriched in forebrain neurons and involved in synaptic regulation. Human genetic studies associated *PTK2B*, the gene coding Pyk2, with risk for Alzheimer's disease (AD). We previously showed that Pyk2 is important for hippocampal function, plasticity, and spine structure. However, its potential role in AD is unknown. To address this question we used human brain samples and 5XFAD mice, an amyloid mouse model of AD expressing mutated human amyloid precursor protein and presenilin1. In the hippocampus of 5XFAD mice and in human AD patients' cortex and hippocampus, Pyk2 total levels were normal. However, Pyk2 Tyr-402 phosphorylation levels, reflecting its autophosphorylation-dependent activity, were reduced in 5XFAD mice at 8 months of age but at 3 months. We crossed these mice with $Pyk2^{-/-}$ mice to generate 5XFAD animals devoid of Pyk2. At 8 months the phenotype of 5XFAD x $Pyk2^{-/-}$ double mutant mice was not different from that of 5XFAD. In contrast, overexpression of Pyk2 in the hippocampus of 5XFAD mice, using adeno-associated virus, rescued autophosphorylated Pyk2 levels and improved synaptic markers and performance in several behavioral tasks. Both $Pyk2^{-/-}$ and 5XFAD mice showed an increase of potentially neurotoxic Src cleavage product, which was rescued by Pyk2 overexpression. Manipulating Pyk2 levels had only minor effects on Aβ plaques, which were slightly decreased in hippocampus CA3 region of double mutant mice and increased following overexpression. Our results show that Pyk2 is not essential for the pathogenic effect of human amyloidogenic mutations in the 5XFAD mouse model. However, the slight decrease in plaque number observed in these mice in the absence of Pyk2 and their increase following Pyk2 overexpression suggest a contribution of this kinase in plaque formation. Importantly, a decreased function of Pyk2 was observed in 5XFAD mice, indicated by its decreased autophosphorylation and associated Src alterations. Overcoming this deficit by Pyk2 overexpression improved the behavioral and molecular phenotype of 5XFAD mice. Thus, our results in a mouse model of AD suggest that Pyk2 impairment may play a role in the symptoms of the disease.

Key words: Alzheimer's disease, mouse model, non-receptor tyrosine protein kinase, Pyk2, Src

List of abbreviations

5XFAD, mice transgenic for human APP and presenilin1 with 5 mutations found in familial Alzheimer's disease
AAV, adeno-associated virus
Aβ, amyloid β
AD, Alzheimer's disease
ANOVA, analysis of variance
APP, amyloid precursor protein
CA1/3, *cornu Ammoni* 1/3
DAPI, 4', 6-diamidine-2'-phenylindole
DG, dentate gyrus
FAK, focal adhesion kinase
GFAP, glial fibrillary acidic protein
GFP, green fluorescent protein
IB, immunoblotting
IF, immunofluorescence
Inserm, Institut national de la santé et de la recherche médicale
LTM, long term memory
LTP, long term potentiation
mGluR5, metabotropic glutamate receptor 5
NIH, National Institute of Health
NMDA, N-methyl-D-aspartate
PLA, proximity ligation assay
PrPc, cellular prion protein
PTK2B, protein tyrosine kinase 2B
Pyk2, proline-rich tyrosine kinase 2
SDS, sodium dodecyl sulfate
SEM, standard error of the mean
SFK Src-family kinase
STEP, striatal enriched phosphatase
STM, short term memory
WT, wild type

Introduction

Late onset Alzheimer's disease (AD) is the most common form of dementia in the aging population accounting for 60–80% of all cases [1]. AD is a progressive neurodegenerative disorder characterized by plaques composed of β-amyloid protein (Aβ) surrounded by dystrophic neurites and neurofibrillary tangles [1]. These histopathological hallmarks are accompanied by synaptic and neuronal loss, cerebral atrophy, cerebral amyloid angiopathy [2], and inflammatory processes [3]. The progression of neurodegeneration in AD patients results in memory impairment and decline in other cognitive abilities often combined with non-cognitive symptoms including mood and personality changes [1].

A meta-analysis of genome-wide association studies identified 11 new loci associated with AD, among which *PTK2B* was one of the most significant [4]. This finding was replicated in other studies [5], which suggested that *PTK2B* was associated with hippocampal sclerosis [6], disease progression [7], and cognitive decline [8]. *PTK2B* encodes Pyk2, a Ca^{2+}-activated non-receptor tyrosine kinase closely related to focal adhesion kinase (FAK) [9-11]. The sensitivity of Pyk2 to increases in intracellular free Ca^{2+} distinguishes it from other tyrosine kinases. In response to Ca^{2+} Pyk2 is autophosphorylated on Tyr-402, which recruits and activates Src-family kinases (SFKs), [12, 13]. In turn, SFKs phosphorylate other residues in Pyk2 and associated proteins, and initiate multiple signaling pathways. The striatal-enriched protein tyrosine phosphatase (STEP), which is enriched in forebrain regions, dephosphorylates Pyk2 [14]. Pyk2 plays a role in several cancers and specific inhibitors are under development [15]. Although many cell types express Pyk2, it is highly enriched in forebrain neurons [16] where it is activated by neuronal activity and excitatory neurotransmission [17-19]. Pyk2 regulates NMDA receptor function and is involved in synaptic plasticity [18, 20, 21]. Our recent work with Pyk2 knockout mice shows that Pyk2 in the hippocampus is essential for spatial memory and long-term potentiation [22]. It also modulates the density and morphology of spines and the organization of post-synaptic regions [22]. Interestingly, heterozygous Pyk2 knockout mice have memory and hippocampal long term potentiation (LTP) deficits similar to homozygous mice and decreased Pyk2 levels contribute to the hippocampal phenotype of a Huntington's disease mouse model [22]. Thus, partial loss of Pyk2 function in the hippocampus has clear functional consequences.

The production of Aβ, a particular proteolytic fragment of amyloid precursor protein (APP), is a hallmark of AD [23]. It can form plaques and neurotoxic oligomers of various conformation and complexity [24]. Aβ oligomers can bind to cellular prion protein (PrPc) [25] and signaling by PrPc and metabotropic glutamate receptor 5 (mGluR5), which includes Pyk2 activation, is disrupted by Aβ oligomers [26]. Another key molecular abnormality in AD is aberrant phosphorylation of Tau [27]. In *Drosophila* the single orthologue of Pyk2 and FAK interacts with Tau and appears to suppress its toxicity [28]. Moreover, in human AD brain hyperphosphorylated Tau and Pyk2 are colocalized [28]. Finally, inhibitors of STEP enhance Pyk2 phosphorylation *in vivo* and improve some cognitive deficits in 3xTg-AD mouse model of AD [29]. Thus, the *PTK2B* locus is reliably associated with AD risk and experimental evidence suggests that Pyk2 has the potential to play a role in the course of the disease, which remains to be characterized.

Here we investigated the role of Pyk2 in the 5XFAD mouse model in which Aβ production is strongly increased, due to expression of mutated forms of human APP and presenilin-1 [30]. These mice display age-dependent plaque development with features of AD including hippocampal-related cognitive deficits, neuroinflammation, neuronal loss, and synaptic degeneration [30]. We tested the potential role of Pyk2 in this model by genetic deletion and adeno-associated virus (AAV) mediated overexpression. Although Pyk2 levels were not changed in samples from AD or 5XFAD mice, Pyk2 autophosphorylation was reduced in 5XFAD mice indicating a decreased function. Deletion of the Pyk2 gene did not markedly alter the phenotype of 5XFAD mice, whereas overexpression of Pyk2 in the hippocampus rescued some behavioral alterations with correction of deficit in synaptic proteins and Src.

Materials and methods

Mouse lines

5XFAD mice expressing human amyloid precursor protein 695 (APP695) with Swedish, London, and Florida mutations, and M146L/L286V presenilin-1, under the control of the murine Thy-1 promoter [30], were crossed with Pyk2$^{-/-}$ mice [31]. Genotyping [30, 31] was carried out from tail biopsy (Charles River services, France). Mice were housed at 19–22ºC and 40–60% humidity

with *ad libitum* access to food and water, under a 12:12 h light/dark cycle and used at 8 months, in accordance with ethical guidelines (Declaration of Helsinki and National Institute of Health, publication no. 85-23, revised 1985, European Community Guidelines, and French Agriculture and Forestry Ministry guidelines for handling animals, decree 87849, license A 75-05-22), approved by the *Charles Darwin* ethical committee. Male and female mice were used.

Human samples

Prefrontal tissue was from patients with AD Braak grades V-VI (3 females, 2 males, age, 87.6 ± 2.8 years; post-mortem intervals, 8.0 ± 2.4 hours, means ± SEM) and control cases (4 females, 1 male, age, 87.2 ± 3.3 years; post-mortem intervals, 7.2 ± 0.9 hours) were obtained from the *Centre de Neurologie Cognitive*, Lariboisière Hospital (Paris France) with approval by the Ethical Committee of Paris University Hospitals (CEERB Bichat University Hospital, Paris, France). Hippocampal samples were obtained from two different sources: i) The Lille Neurobank (fulfilling criteria of the French law on biological resources and declared to competent authority under the number DC-2008-642) with donor consent, data protection and ethical committee review, samples managed by the CRB/CIC1403 Biobank, BB-0033-00030, patients with AD Braak stage VI (3 females, 2 males, age, 75.4 ± 3.8 years, post-mortem interval 17.4 ± 3.8 h, means ± SEM) and controls (2 females, 3 males, age, 50.8 ± 9.7 years, post-mortem interval 16.6 ± 4.0 h); ii) the Banc de Teixits Neurològics (Biobanc-HC-IDIBAPS) with the approval of the ethical committee of the University of Barcelona with the reference: IRB00003099, patients with AD Braak grades V-VI (11 females, 4 males, age, 84.7 ± 1.8 years; post-mortem intervals, 9 ± 3.4 hours, means ± SEM) and control cases (6 females, 4 males, age, 84.2 ± 3.4 years; post-mortem intervals, 12 ± 1 hours). The 2 sets of samples were analyzed separately, results expressed as a % of the control mean in the series and data being similar they were pooled for final comparison (1 aberrant point was discarded). All the patients had an history of progressive dementia and satisfied National Institute of Neurological and Communicative Disorders and Stroke–Alzheimer's Disease and Related Disorders (NINCDS-ADRDA) criteria for probable AD [32] and satisfied neuropathological criteria for AD [33]. This research project was.

Tissue preparation and immunoblotting

Brains were quickly removed from mice deeply anesthetized in a CO_2 chamber, hippocampus dissected out, frozen in dry ice, and stored at -80ºC until use. Briefly, tissue was sonicated in 250

µL of lysis buffer (phosphate buffered saline [PBS, NaCl, 137 mM, KCl, 2.7 mM, Na_2HPO4, 10 mM, $KH2PO_4$, 1.8 mM, pH 7.5] with 1% Nonidet P40 [vol/vol], 1 g/L sodium dodecylsulfate (SDS), 5 g/L sodium deoxycholate, protease inhibitors 1:1, 000 [Sigma], and 2 g/L sodium orthovanadate), centrifuged at 15, 000 x g for 20 min and 15 mg protein from the supernatant were analyzed by SDS-polyacrylamide gel electrophoresis (7.5 g/L acrylamide) and transferred to nitrocellulose membranes (Millipore, Bedford, MA). Human tissue was analyzed similarly. Membranes were blocked in TBS-T (150 mM NaCl, 20 mM Tris-HCl, pH 7.5, 0.5 mL/L Tween 20) with 50 g/L non-fat dry milk and 50 g/L BSA, and incubated overnight at 4ºC with shaking, in the presence of primary antibodies in PBS with 0.2 g/L NaN_3 (Supplementary Table 1). After several washes in TBS-T, blots were incubated with anti-rabbit IgG IRdye800CW-coupled or antimouse IgG IRdye700DXcoupled antibodies (1/2, 000, Rockland Immunochemicals, USA) and signal detected by the Odyssey Li-Cor and analyzed using ImageJ.

Immunofluorescence

For immunofluorescence (IF), deeply anesthetized mice (pentobarbital 60 mg/kg) were intracardially perfused with a paraformaldehyde solution (40 g/L paraformaldehyde in 0.12 M sodium phosphate, pH 7.2). Brains were removed and post-fixed overnight in the same solution, cryoprotected with 300 g/L sucrose in PBS with 0.2 g/L NaN_3 and frozen in dry ice-cooled isopentane. Serial coronal 30-µm cryostat sections were free-floating incubated as described [22]. They were washed three times in PBS, permeabilized 15 min at RT in PBS containing 3 mL/L Triton X-100 and 30 mL/L goat serum (Pierce Biotechnology, Rockford, IL). After these washes, brain sections were incubated overnight at 4°C with primary antibodies (antibodies sources and dilutions in Supplementary Table 1) in PBS with 0.2 g/L NaN_3. After three washes sections were incubated 2 h at RT with fluorescent secondary 488 anti-rabbit or 555 anti-mouse antibodies (1:250, Molecular Probes, Sunnyvale, CA). No signal was detected in control sections incubated in the absence of primary antibody. Confocal images were acquired with a Leica Confocal SP5-II (63× numerical aperture lens, 5× digital zoom, 1-Airy unit pinhole, 4-frame averaging per *z*-step, *z*-stacks every 2 µm, 1, 024×1, 024 pixel resolution). PSD95- and synaptophysin-1-positive clusters[34] were analyzed with NIH ImageJ, in at least 3 slices per mouse and up to 3 CA1 *stratum radiatum* images per slice. Stained β-amyloid plaques were photographed from the entire hippocampus (three slices per mouse) with a DM6000-2 microscope (Leica), analyzed with ImageJ and counted manually in CA1, CA3, and DG.

Proximity ligation assay

Proximity ligation assay (PLA) was carried out using Duolink® detection kit (Sigma) according to manufacturer's protocol. Floating-sections were incubated with primary Pyk2 and β-amyloid antibodies overnight at 4°C. PLA probes anti-mouse PLUS and anti-rabbit MINUS were added overnight at 4°C. Sections were washed in TBS + 0.1% Tween 20 and incubated in Duolink® ligation solutions and ligase for 1 h at 37°C. Next, the signal was amplified by the addition of Duolink® amplification and polymerase for 2.5 h at 37°C. The detection of the red fluorophore (excitation 594 nm, emission 624 nm) was used. Nuclei were stained with DAPI using mounting media provided in the kit. As a negative control, one of the two primary antibodies was omitted.

Behavioral tests

Mouse anxiety was analyzed in a plastic elevated plus-maze made with two opposing 30 × 8 cm open arms, and two opposing 30 × 8 cm arms enclosed by 15 cm-high walls placed 50 cm above the floor and dimly lit (60 lux). Each mouse was placed in the central square, facing an open arm and the time spent in the open arms, which normally correlates with low levels of anxiety, measured for 5 minutes.

Spontaneous locomotor activity was measured in dim lit (60 lux) open field white square arena (40 x 40 x 40 cm in length, width, and height respectively). Animals were placed at the center and allowed to explore freely for 30 min. Spontaneous locomotor activity was measured.

Novel object recognition was tested in a dimly lit (60 lux) 40 x 40 x 40 cm white square arena. Mice were first habituated to the arena in the absence of objects (3 days, 15 min/day). On the fourth day, two similar objects were presented to each mouse during 10 min (A′A″ condition) after which they were returned to their home cage for 15 min. After that, the animals were placed in the arena where they were tested during 5 min with a familiar and a new object (A′ B condition; short-term memory, STM), and then returned to their home cage. Twenty-four hours later, the same animals were re-tested for 5 min in the arena with a familiar and a new object (BC condition; long-term memory, LTM). The object preference was measured as the time spent exploring each object × 100/time exploring both objects.

The passive avoidance (light-dark) paradigm was conducted in a 2-compartment box, where 1 compartment was dimly lit (20 lux) and the other brightly lit (200 lux). Both chambers were

connected by a door (5 cm × 5 cm). During training, mice were placed into the aversive brightly lit compartment, and upon the entry into the preferred dimly lit compartment (with all 4 paws inside the dark chamber), they received a mild foot shock (2-second foot shock, 1 mA intensity). The latency of mice to enter into the dark chamber was recorded. Twenty seconds after receiving the foot shock, mice were returned to the home cage until testing 24 hours later (long-term memory). For this retention test, mice were returned to the brightly lit compartment and the latency to enter the shock-paired compartment (dark chamber) was measured (10-min time cutoff).

For all tests at the end of each trial, any defecation was removed and the apparatus was wiped with 30% ethanol. Animals were tracked and recorded with SMART junior software (Panlab, Spain).

Viral constructs and stereotactic injection

For Pyk2 overexpression we used adeno-associated viruses (AAV) expressing Pyk2 [22] (AAV1-CamKIIα (0.4)-GFP-2A-mPTK2B; Vector Biolabs Malvern, PA, USA) or, as control, AAVs expressing GFP (AV-9-PV1917, AAV9.CamKIIα (0.4).eGFP.WPRE.rBG (AAV-GFP) from Perelman School of Medicine, University of Pennsylvania). Mice were anesthetized with pentobarbital (30 mg/kg) and bilaterally injected with AAV-GFP or AAV-Pyk2 (2.06×10^9 GS) in the dorsal hippocampus at the following coordinates from the bregma (millimeters); anteroposterior, –2.0; lateral, +/-1.5; and dorsoventral, -1.4 and -2.0. AAVs were injected over 2 minutes, leaving the cannula in place for 5 additional minutes to ensure complete diffusion of the viruses, and then slowly retracted from the brain. The animals were monitored for 2 hours after administration and then returned to the housing facility for 21 days before behavioral assessment and brain analysis.

Statistical analysis

Analysis was done using GraphPad Prism version 6.00 for Windows, GraphPad Software, La Jolla California USA. Data are expressed as mean + SEM. Normal distribution was tested with d'Agostino and Pearson omnibus, Shapiro-Wilk, and Kolmogorov-Smirnov normality tests. If at least one of them was passed, statistical analysis was performed using two-tailed Student's t-test or ANOVA and Holm-Sidak's *post hoc* test. Otherwise non-parametric Mann and Whitney or Kruskal-Wallis' and Dunn's tests were used. $p < 0.05$ was considered as statistically significant.

Results

Pyk2 expression and phosphorylation in patients and 5XFAD mice

We first examined Pyk2 protein levels in post-mortem prefrontal and hippocampal human tissue. In the two regions Pyk2 levels did not differ between AD patients and controls (**Fig. 1A-B**). The detection of the autophosphorylated form of Pyk2 in the human brain samples, either in patients or in controls, was variable from one batch to the other, presumably due to post-mortem endogenous dephosphorylation (not shown) making this measurement unreliable. We then analyzed the hippocampus of 8-month-old 5XFAD mice, at an age at which they have a clear phenotype [30, 35] to be comparable to the human samples. Total Pyk2 levels were similar in wild type (WT) and 5XFAD mice, whereas pTyr402-Pyk2 levels were lower in 5XFAD than in WT mice (**Fig. 1C-D**). Since autophosphorylation at Tyr402 is a key step in the activation of Pyk2 [12, 36, 37] this result indicated a functional alteration of this kinase. In contrast, in 3-month-old 5XFAD mice, both total Pyk2 and pTyr402-Pyk2 levels were similar to WT (**Fig. 1C, E**). Our results show that Pyk2 levels were normal in AD patients and 5XFAD mice but that its autophosphorylation was decreased in 8-month 5XFAD mice.

Pyk2 is co-localized with Aβ in 5XFAD mice

We compared Pyk2 localization in the hippocampus of 5XFAD mice with Aβ immunoreactivity and plaques. Aβ-positive plaques were negative for Pyk2 (**Fig. 2A-C**). In contrast, Pyk2 and Aβ-like immunofluorescence displayed a significant degree of colocalization in neuropil zones devoid of amyloid plaques (**Fig. 2D**), as supported by the calculation of the Manders' colocalization coefficient [38] in the 3 hippocampal regions studied (**Fig. 2E**). To corroborate this

apparent colocalization, we used an *in situ* proximity ligation assay (PLA). Hippocampal sections of 5XFAD mice were probed with Pyk2 and β-amyloid antibodies followed by hybridization with secondary antibodies coupled to oligonucleotides that hybridize together if the distance between the two target proteins is <40 nm. The interaction between Pyk2 and β-amyloid was detected as red dots in all hippocampal regions (**Fig. 2F**, right panels). As a negative control, only one primary antibody was added and amplification of the signal was not detected (**Fig. 2F**, left panels). These results provide evidence for some degree of colocalization of Pyk2 and Aβ immunoreactivity in the neuropil of 5XFAD mice.

Pyk2 genetic deletion does not change the behavioral phenotype of 5XFAD mice

We reasoned that if Pyk2 played a role in the pathogenesis of the 5XFAD model, its deletion should delay or modify their phenotype. We crossed 5XFAD mice with Pyk2$^{-/-}$ mice and studied their phenotype at 8-month, an age at which these mice have a clear but not severe behavioral phenotype [22]. We focused on a single time point, since the relatively mild phenotype was appropriate to detect either improvement or worsening of the disease. We compared WT and 5XFAD mice, expressing or not Pyk2 (**Fig. 3A**). All mice displayed similar spontaneous locomotor activity (**Fig. 3B**). To study memory capabilities, since Pyk2 deletion by itself impairs hippocampus-dependent spatial memory [22], we used the novel object recognition test, which was not impaired in Pyk2$^{-/-}$ mice (**Fig. 3C-D**). Twenty min after training, mice of all genotypes preferentially explored the novel object (short-term memory, **Fig. 3C**). One day after object displacement, WT and Pyk2$^{-/-}$ mice still explored more the new object than the familiar one (**Fig. 3D**). In contrast this preference was completely absent in both 5XFAD and 5XFAD x Pyk2$^{-/-}$ mice, revealing a specific long-term memory deficit in 5XFAD, which was not modified in the absence of Pyk2$^{-/-}$ (**Fig. 3D**). We next examined associative memory in the passive avoidance task (**Fig. 3E**). Latency to step-through during the training session was similar in the 4 genotypes. In the testing session, 24 hours later, although all mice showed a pronounced increase in the latency to enter the dark compartment, this latency was lower in 5XFAD, Pyk2$^{-/-}$, and 5XFAD x Pyk2$^{-/-}$ mice than in WT littermates (**Fig. 3E**). These results showed that Pyk2 deletion induced by itself a deficit in the passive avoidance performance, and that this deficit was not additive with the alterations observed in 5XFAD mice. Finally, we used the elevated plus-maze to evaluate

anxiety, which is decreased in 5XFAD mice [35, 39]. As expected, 5XFAD mice spent more time in the open arms than their WT littermates (**Fig. 3F**). Pyk2$^{-/-}$ mice did not differ from WT mice, nor 5XFAD x Pyk2$^{-/-}$ from 5XFAD (**Fig. 3F**). Taken together these results confirm the existence of behavioral alterations in 5XFAD mutant mice, which were not modified in the absence of Pyk2.

Pyk2 knockout induces only minor changes in 5XFAD mice neuropathology

The number of synapses decreases in 5XFAD mice in correlation with cognitive decline [39-41]. To examine whether this alteration was modified in the absence of Pyk2, we measured immunoreactive puncta for PSD95 and synaptophysin, which are post- and pre- synaptic markers, respectively, and which have been previously used in AD mouse models as an indication of the number of synapses [39-41]. We analyzed these two markers in CA1 *stratum radiatum* of 8-month mice (**Fig. 4A-D**). PSD-95-positive puncta were decreased in CA1of Pyk2$^{-/-}$ mice, as previously described [22], and in 5XFAD mice [39-41], as well as in the double mutants (**Fig. 4A-B**). The lack of additivity of the defect on the double mutants suggested that the post-synaptic alteration of PSD-95 might depend on common molecular dysfunction in the two mutant mice. In contrast, synaptophysin-positive puncta were decreased in 5XFAD but not Pyk2$^{-/-}$ hippocampus (**Fig. 4C-D**), consistent with the predominantly post-synaptic phenotype in Pyk2 KO mice [22].

To test whether the lack of Pyk2 can exacerbate or ameliorate β-amyloidosis in 8-month 5XFAD mice we then counted the number of Aβ-immunoreactive plaques in three regions of dorsal hippocampus (CA1, CA3, and dentate gyrus, DG) in 5XFAD and 5XFAD x Pyk2$^{-/-}$ mice (**Fig. 4E-F**). Although hippocampal plaque load was similar in the two genotypes in CA1 and DG, the number of plaques was decreased in CA3 of 5XFAD x Pyk2$^{-/-}$ mice as compared to 5XFAD littermates. Hippocampal levels of glial fibrillary acidic protein (GFAP), an index of astrogliosis, were similar in WT and Pyk2$^{-/-}$ mice and were increased in both 5XFAD and 5XFAD x Pyk2$^{-/-}$ mice (**Fig. 4G-H**). In summary, the absence of Pyk2 did not further modify the synaptic markers, the amyloid plaques or astrogliosis in 5XFAD mice, except for a decrease in the number of plaques in CA3.

Pyk2 overexpression in dorsal hippocampus partially improves the behavioral phenotype of 5XFAD mice

Since the absence of Pyk2 did not markedly modify the phenotype of 5XFAD mice, it was unlikely that it played a necessary role in the pathogenesis in this model. We therefore hypothesized that, on the contrary, the functional Pyk2 deficit observed in 5XFAD mice might be involved in their phenotype. To test this hypothesis, since there is no means to stimulate Pyk2 directly, we decided to increase its expression levels. Eight-month-old WT and 5XFAD mice received in the dorsal hippocampus a bilateral stereotactic injection of AAV expressing Pyk2 (5XFAD/Pyk2 mice) or GFP (WT/GFP and 5XFAD/GFP), as a control (**Fig. 5A**). Three weeks later, Pyk2 protein levels increased in 5XFAD/Pyk2 mice as compared to WT/GFP and 5XFAD/GFP mice (**Fig. 5B-C**). The overall increase in total hippocampal Pyk2 levels was 73% and the increase in pTyr402-Pyk2 levels was 51%, sufficient to restore its levels slightly above those in WT/GFP controls (**Fig. 3B-D**). We thus, expected to rescue autophosphorylation-dependent functions of Pyk2. We then carried out the same set of behavioral tests in these mice as in Pyk2 KO mice (see **Fig. 3**). In the elevated plus-maze (**Fig. 5E**) the increased time spent in the open arms by 5XFAD/GFP mice, compared with WT/GFP mice, was corrected in 5XFAD/Pyk2 mice. Locomotor activity in the open field was similar in all groups of AAV-injected mice (**Fig. 5F**). In the passive avoidance test no difference was observed between 5XFAD/GFP and 5XFAD/Pyk2 mice (**Fig. 5G**), showing that, as expected, overexpression of Pyk2 in the hippocampus was not sufficient to restore the associative memory evaluated in this paradigm that also involves other brain regions. As observed above (**Fig. 3C**), the three groups of mice did not display any deficit in short-term memory in the novel object recognition test (**Fig. 5H**). However, the deficit in long-term memory observed in 5XFAD/GFP mice, as compared to WT/GFP, was restored in 5XFAD/Pyk2 mice (**Fig. 5I**). Thus, behavioral evaluation showed that overexpression of Pyk2 in the dorsal hippocampus of 5XFAD mice rescued some deficits including impairment in long-term memory in the novel object recognition test and aberrant performance in the elevated plus-maze.

Pyk2 overexpression in dorsal hippocampus increases the number of plaques but rescues the loss of synaptic markers in CA1 of 5XFAD mice

To test whether Pyk2 overexpression in the hippocampus modified β-amyloidosis we counted the number of Aβ-immunofluorescent plaques in the hippocampus in 8-month 5XFAD/GFP and 5XFAD/Pyk2 mice (**Fig. 6A**, **B**). The plaque number in all three regions studied was higher in 5XFAD/Pyk2 than in 5XFAD/GFP mice by 50-60%. In contrast, GFAP levels were increased to similar levels in 5XFAD/GFP and 5XFAD/Pyk2 mice as compared to WT/GFP (**Fig. 6C-D**), indicating that astrogliosis was similar in the three groups of mice. In summary, hippocampal overexpression of Pyk2 in 5XFAD mice increased the number of Aβ plaques in the hippocampus.

Since the moderate increase in Aβ-plaque load in Pyk2 overexpressing mice contrasted with the partial behavioral improvement, we studied possible improvements of other parameters, focusing on synaptic markers. We examined the PSD95-immunoreactive and synaptophysin-immunoreactive puncta (post- and pre- synaptic markers, respectively), which are an indication of the number of synapses and are decreased in 5XFAD mice in correlation with cognitive decline [39-41]. We analyzed these two markers in CA1 *stratum radiatum* of 8-month mice. As expected and as observed above for mice from the same genotypes (see **Fig. 4A-D**), the number of PSD-95-positive and synaptophysin-positive puncta was decreased in 5XFAD/GFP as compared to WT/GFP mice (**Fig. 6E-H**). The PSD-95 decrease was rescued in 5XFAD/Pyk2 mice and the synaptophysin alteration was partly corrected (**Fig. 6F, H**). These results suggest that the behavioral improvement observed in 5XFAD mice following hippocampal overexpression of Pyk2 was accompanied by an improvement in the number of synapses revealed by both pre- and post-synaptic markers.

Role of Pyk2 in Src cleavage in 5XFAD mice

Since Pyk2 phosphorylation on Tyr-402 was decreased in 5XFAD mice, we examined Src-family kinases (SFKs), which are recruited and activated when Pyk2 is autophosphorylated at this residue [12]. We have previously shown that SFKs autophosphorylation is decreased in $Pyk2^{-/-}$ mice [22]. Here we measured the total amount of Src in the hippocampus of $Pyk2^{-/-}$ mice by immunoblotting. Src full-length form (66 kDa) was decreased, whereas a 52-kDa fragment, detected by an antibody that recognizes a C-terminal epitope, was increased in $Pyk2^{+/-}$ and $Pyk2^{-/-}$ mice (**Fig. 7A-B**). Both changes were gene-dosage-dependent (**Fig. 7B**). These results on Src contrasted with our previous observations on Fyn, which did not appear to be altered in Pyk2

mutant mice [22] and indicated the existence of a proteolytic cleavage of Src in the absence of Pyk2. Interestingly, a similar 52-kDa cleaved Src with potential neurotoxic properties has been reported following excitotoxic stimuli and ischemia [42], suggesting a possible pathogenic role. We therefore studied Src in 5XFAD mice as compared to WT and found that the 52-kDa form of Src was also increased (**Fig. 7C-D**). We then measured the two forms of Src in WT, Pyk2$^{-/-}$, 5XFAD, and double mutant mice (**Fig. 7E-F**). In this experiment the decrease in 66-kDa Src was not observed in Pyk2$^{-/-}$ mice, indicating variability of this parameter. In contrast, the 52-kDa form was reproducibly increased in Pyk2$^{-/-}$, 5XFAD, and double mutant mice (**Fig. 7E-F**). We repeated this experiment in AAV-injected mice and observed again an increase in 52-kDA Src, which was corrected by AAV-mediated Pyk2 expression (**Fig. 7D, E**). Taken together these results indicate that a decrease in Pyk2 levels and/or autophosphorylation can trigger the appearance of a shorter form of Src, presumably corresponding to a cleaved form missing the N-terminal fragment, with potentially cytotoxic properties. This fragment may contribute to the consequences of Pyk2 decreased function (autophosphorylation) in the 5XFAD model.

Discussion

Although *PTK2B* is genetically associated with late onset AD [4-6], we do not know whether and how Pyk2, the tyrosine kinase coded by this gene, is involved in the disease. By crossing 5XFAD mice, a transgenic mouse model that mimics human amyloidogenic pathway alterations [30], with Pyk2 *knockout* mice we observed that the absence of Pyk2 did not dramatically alter the neurological phenotype of 5XFAD mice. This showed that Pyk2 is not essential for the deleterious consequences of increased Aβ production. The only difference we detected in comparison to simple 5XFAD mice was a decrease in the number of plaques in CA3, indicating a possible contribution of Pyk2 in their appearance. We did not find any major change in Pyk2 protein levels in cortical or hippocampal samples from human AD patients or in 5XFAD mouse hippocampus. However, in 8-month 5XFAD mice Pyk2 autophosphorylation site, Tyr402, was less phosphorylated than in WT littermates, indicating an alteration of Pyk2 activation. In younger animals (3-month) basal levels of pTyr402-Pyk2 were normal, indicating that Pyk2 autophosphorylation deficit is not a very early alteration. Although the cause of Pyk2 functional deficit in 5XFAD mice is not known, it has been shown that Pyk2 is activated downstream of a

complex associating PrPc and mGluR5 glutamate receptors, and that this activation is disrupted by Aβ oligomers [26]. Such disruption might contribute to Pyk2 functional deficit.

To test whether decreased Pyk2 activity in these mice could contribute to their memory deficit we overexpressed Pyk2 in the dorsal hippocampus and thus corrected the levels of autophosphorylated Pyk2. This strategy improved some aspects of the behavioral phenotype, including performance in the elevated plus-maze and novel object recognition long-term memory. Pyk2 overexpression also improved synaptic alterations which are known to be a major source of AD symptomatology [43-45]. In support of a role of Pyk2 at synapses, recent evidence shows that Pyk2 plays an important role at hippocampal synapses [22]. Pyk2 is involved in PSD-95 post-synaptic recruitment and clustering [22], regulates NMDA receptors subunits [18, 22] and even the 50% Pyk2 decrease observed in heterozygous Pyk2+/- mice is sufficient to markedly alter synaptic properties [22]. The behavioral improvement induced by Pyk2 overexpression in 5XFAD mice was associated with a pronounced reduction of previously reported synaptic alterations [39, 40], evidenced by the recovery of PSD-95 and synaptophysin clustering. We therefore suggest that Pyk2 functional deficit in 5XFAD mice contributes to the synaptic alterations and that its rescue is an important contribution to Pyk2-induced behavioral improvement.

One of the mechanisms possibly linking Pyk2 deficiency with synaptic dysfunction is a deficit in SFK activation. We previously reported a decreased SFK basal autophosphorylation in the hippocampus of Pyk2 knockout mice with no change in total levels of Fyn [22]. We show here that Pyk2 mutant mice display increased levels of a smaller 52-kDa form of Src. This observation is reminiscent of the reported cleavage of Src by calpain, a Ca^{2+}-activated protease, which generates a ~52 kDa protein lacking the N-terminal myristoylation site [42]. This truncated Src is generated *in vivo* following ischemia and has neurotoxic properties [42]. In 5XFAD mice although modifications of full-length Src were not detected, the 52-kDa fragment was increased, and Pyk2 overexpression corrected this alteration, possibly alleviating a toxic effect. It can be therefore hypothesized that this Src fragment could contribute to the impairments in 5XFAD mice. The mechanisms leading to the putative cleavage of Src in Pyk2 mutant and 5XFAD mice are not known and will require further exploration.

Our work reveals the multiple roles that SFKs appear to have in AD models. On the one hand, several studies showed that Fyn inhibition either genetically [46, 47] (but see [48]) or using pharmacological inhibition of Fyn [49, 50] improves their phenotype, possibly in relation with a contribution of Fyn to Tau pathology at the somatodendritic level [49, 51, 52]. On the other hand, our results indicate that a deficit in SFK activation, possibly at the synaptic level, may also contribute to functional deficits in Pyk2 mutant mice and in 5XFAD mice. A toxic Src breakdown product may have an additional negative role. Thus Pyk2 through its capacity to recruit and activate SFKs in response to neuronal activity is strategically located to modulate the balance between their various implications. Importantly, this role of Pyk2 deficit in 5XFAD mice phenotype fully agrees with the observation that inhibition of STEP, a phosphatase active on Pyk2 [14], increases Pyk2 phosphorylation and improves the behavior of 3xTg-AD mice [29].

The complexity of the role of Pyk2 and SFKs in the context of AD is also illustrated by their possible contribution to amyloidogenesis. SFKs have been reported to contribute to Aβ increase production [53, 54]. In our study manipulating Pyk2 levels in vivo had only moderate effects on the number plaques, which were opposite to the functional and synaptic improvements. In the absence of Pyk2, we found a decrease in amyloid plaques in CA3, whereas Pyk2 overexpression in 5XFAD mice slightly increased plaque number throughout the hippocampus. These results suggest that Pyk2 might contribute to plaque formation, possibly through a modulation of Aβ production. In this respect it is interesting to note that Pyk2- and Aβ-like immunoreactivities colocalized in the neuropil but not in plaques, indicating a proximity of Pyk2 with sites of Aβ production. In our experimental conditions, however, the changes in plaque numbers were in opposite direction to the observed behavioral improvement, suggesting they did not play a major role in the overall effect of Pyk2 in the 5XFAD model. It should be noted that although a decrease in plaque number is usually correlated with behavioral improvement in 5XFAD mice [55-58], the role of plaques by themselves in the disease is disputed [59, 60]. It is also possible that the strong effect of mutations responsible for Aβ production in 5XFAD mice partly occluded the contribution of Pyk2 to amyloid production and revealed the prominent impact of Pyk2 deficit in synaptic dysfunction.

In summary, we have explored the potential role of Pyk2 in a transgenic amyloid mouse model of AD. Our results do not support a strong positive or negative role of Pyk2 in this model

of the disease. In contrast, they indicate a functional deficit of Pyk2 that is likely to contribute to synaptic alterations and to generation of a potentially toxic Src fragment. In 5XFAD mice, enhancing Pyk2 function by overexpression corrects these various alterations and has an overall beneficial effect on behavior, suggesting that restoring Pyk2 might be a useful target in AD.

Declarations

Ethics approval

The use of human samples was approved by the Ethical Committee of Paris University Hospitals (CEERB Bichat University Hospital, Paris, France). Mouse experiments were approved by the Charles Darwin ethical committee.

Competing interests

The authors have no competing financial interest to declare.

Funding

This work was supported in part by Inserm, *Sorbonne-Université* (formerly *Université Pierre et Marie Curie,* UPMC, Paris-6), and grants from ANR MALZ-2013 to JH and JAG, the King Abdullah University of Science and Technology (KAUST) Office of Sponsored Research award (#OSR-2015-CRG4-2602) to SA and JAG, and Ministerio de Ciencia e Innovación (SAF2015-67474-R;MINECO/FEDER to SG. Equipment at the IFM was also supported by DIM NeRF from *Région Ile-de-France* and by the FRC/Rotary "Espoir en tête". AG is a Ramón y Cajal fellow (RYC-2016-19466).

Authors' contributions

AG designed and carried out experiments, analyzed results and wrote the manuscript, BdP, CCD, LLM, ATF, and MT carried out experiments, VD provided material, SG, SA and JH provided expertise and reagents, and participated in the design of the study and the writing of the manuscript, JAG designed and supervised the study, analyzed results and wrote the manuscript.

Acknowledgements.

The Girault's lab is affiliated with the Paris School of Neuroscience (ENP) and the "Biology for Psychiatry" laboratory of excellence "Bio-Psy labex". Imaging was carried out at the *Institut du Fer à Moulin* "Cell and Tissue Imaging facility". We are grateful to the Banc de Teixits Neurològics (Biobanc-HC-IDIBAPS) for providing brain samples from control subjects and AD patients.

References

1. Alzheimer's Association Report 2012 Alzheimer's disease facts and figures. Alzheimers Dement. 2012;8:131-168.
2. Vinters HV: Emerging concepts in Alzheimer's disease. Annu Rev Pathol. 2015;10:291-319.
3. Heneka MT, Carson MJ, El Khoury J, Landreth GE, Brosseron F, Feinstein DL, Jacobs AH, Wyss-Coray T, Vitorica J, Ransohoff RM, et al: Neuroinflammation in Alzheimer's disease. Lancet Neurol. 2015;14:388-405.
4. Lambert JC, Ibrahim-Verbaas CA, Harold D, Naj AC, Sims R, Bellenguez C, DeStafano AL, Bis JC, Beecham GW, Grenier-Boley B, et al: Meta-analysis of 74, 046 individuals identifies 11 new susceptibility loci for Alzheimer's disease. Nat Genet. 2013;45:1452-1458.
5. Jiao B, Liu X, Zhou L, Wang MH, Zhou Y, Xiao T, Zhang W, Sun R, Waye MM, Tang B, Shen L: Polygenic Analysis of Late-Onset Alzheimer's Disease from Mainland China. PLoS One. 2015;10:e0144898.
6. Beecham GW, Hamilton K, Naj AC, Martin ER, Huentelman M, Myers AJ, Corneveaux JJ, Hardy J, Vonsattel JP, Younkin SG, et al: Genome-wide association meta-analysis of neuropathologic features of Alzheimer's disease and related dementias. PLoS Genet. 2014;10:e1004606.
7. Wang X, Lopez OL, Sweet RA, Becker JT, DeKosky ST, Barmada MM, Demirci FY, Kamboh MI: Genetic determinants of disease progression in Alzheimer's disease. J Alzheimers Dis. 2015;43:649-655.
8. Nettiksimmons J, Tranah G, Evans DS, Yokoyama JS, Yaffe K: Gene-based aggregate SNP associations between candidate AD genes and cognitive decline. Age (Dordr). 2016;38:41.
9. Lev S, Moreno H, Martinez R, Canoll P, Peles E, Musacchio JM, Plowman GD, Rudy B, Schlessinger J: Protein tyrosine kinase PYK2 involved in Ca(2+)-induced regulation of ion channel and MAP kinase functions. Nature. 1995;376:737-745.
10. Sasaki H, Nagura K, Ishino M, Tobioka H, Kotani K, Sasaki T: Cloning and characterization of cell adhesion kinase beta, a novel protein-tyrosine kinase of the focal adhesion kinase subfamily. J Biol Chem. 1995;270:21206-21219.
11. Avraham S, London R, Fu Y, Ota S, Hiregowdara D, Li J, Jiang S, Pasztor LM, White RA, Groopman JE, et al.: Identification and characterization of a novel related adhesion focal tyrosine kinase (RAFTK) from megakaryocytes and brain. J Biol Chem. 1995;270:27742-27751.
12. Dikic I, Tokiwa G, Lev S, Courtneidge SA, Schlessinger J: A role for Pyk2 and Src in linking G-protein-coupled receptors with MAP kinase activation. Nature. 1996;383:547-550.
13. Walkiewicz KW, Girault JA, Arold ST: How to awaken your nanomachines: Site-specific activation of focal adhesion kinases through ligand interactions. Prog Biophys Mol Biol. 2015;119:60-71.
14. Xu J, Kurup P, Bartos JA, Patriarchi T, Hell JW, Lombroso PJ: Striatal-enriched protein-tyrosine phosphatase (STEP) regulates Pyk2 kinase activity. J Biol Chem. 2012;287:20942-20956.

15. Lipinski CA, Loftus JC: Targeting Pyk2 for therapeutic intervention. Expert Opin Ther Targets. 2010;14:95-108.
16. Menegon A, Burgaya F, Baudot P, Dunlap DD, Girault JA, Valtorta F: FAK+ and PYK2/CAKbeta, two related tyrosine kinases highly expressed in the central nervous system: similarities and differences in the expression pattern. Eur J Neurosci. 1999;11:3777-3788.
17. Corvol JC, Valjent E, Toutant M, Enslen H, Irinopoulou T, Lev S, Herve D, Girault JA: Depolarization activates ERK and proline-rich tyrosine kinase 2 (PYK2) independently in different cellular compartments in hippocampal slices. J Biol Chem. 2005;280:660-668.
18. Huang Y, Lu W, Ali DW, Pelkey KA, Pitcher GM, Lu YM, Aoto H, Roder JC, Sasaki T, Salter MW, MacDonald JF: CAKbeta/Pyk2 kinase is a signaling link for induction of long-term potentiation in CA1 hippocampus. Neuron. 2001;29:485-496.
19. Siciliano JC, Toutant M, Derkinderen P, Sasaki T, Girault JA: Differential regulation of proline-rich tyrosine kinase 2/cell adhesion kinase beta (PYK2/CAKbeta) and pp125(FAK) by glutamate and depolarization in rat hippocampus. J Biol Chem. 1996;271:28942-28946.
20. Bartos JA, Ulrich JD, Li H, Beazely MA, Chen Y, Macdonald JF, Hell JW: Postsynaptic clustering and activation of Pyk2 by PSD-95. J Neurosci. 2010;30:449-463.
21. Hsin H, Kim MJ, Wang CF, Sheng M: Proline-rich tyrosine kinase 2 regulates hippocampal long-term depression. J Neurosci. 2010;30:11983-11993.
22. Giralt A, Brito V, Chevy Q, Simonnet C, Otsu Y, Cifuentes-Díaz C, de Pins B, Coura R, Alberch J, Ginés S, et al: Pyk2 modulates hippocampal excitatory synapses and contributes to cognitive deficits in a Huntington's disease model. Nat Commun. 2017;8:15592.
23. Benilova I, Karran E, De Strooper B: The toxic Abeta oligomer and Alzheimer's disease: an emperor in need of clothes. Nat Neurosci. 2012;15:349-357.
24. Mucke L, Selkoe DJ: Neurotoxicity of amyloid beta-protein: synaptic and network dysfunction. Cold Spring Harb Perspect Med. 2012;2:a006338.
25. Lauren J, Gimbel DA, Nygaard HB, Gilbert JW, Strittmatter SM: Cellular prion protein mediates impairment of synaptic plasticity by amyloid-beta oligomers. Nature. 2009;457:1128-1132.
26. Haas LT, Strittmatter SM: Oligomers of Amyloid beta Prevent Physiological Activation of the Cellular Prion Protein-Metabotropic Glutamate Receptor 5 Complex by Glutamate in Alzheimer Disease. J Biol Chem. 2016;291:17112-17121.
27. Mandelkow EM, Mandelkow E: Biochemistry and cell biology of tau protein in neurofibrillary degeneration. Cold Spring Harb Perspect Med. 2012;2:a006247.
28. Dourlen P, Fernandez-Gomez FJ, Dupont C, Grenier-Boley B, Bellenguez C, Obriot H, Caillierez R, Sottejeau Y, Chapuis J, Bretteville A, et al: Functional screening of Alzheimer risk loci identifies PTK2B as an in vivo modulator and early marker of Tau pathology. Mol Psychiatry. 2016.
29. Xu J, Chatterjee M, Baguley TD, Brouillette J, Kurup P, Ghosh D, Kanyo J, Zhang Y, Seyb K, Ononenyi C, et al: Inhibitor of the tyrosine phosphatase STEP reverses cognitive deficits in a mouse model of Alzheimer's disease. PLoS Biol. 2014;12:e1001923.
30. Oakley H, Cole SL, Logan S, Maus E, Shao P, Craft J, Guillozet-Bongaarts A, Ohno M, Disterhoft J, Van Eldik L, et al: Intraneuronal beta-amyloid aggregates, neurodegeneration, and neuron loss in transgenic mice with five familial Alzheimer's

disease mutations: potential factors in amyloid plaque formation. J Neurosci. 2006;26:10129-10140.
31. Giralt A, Coura R, Girault JA: Pyk2 is essential for astrocytes mobility following brain lesion. Glia. 2016;64:620-634.
32. McKhann G, Drachman D, Folstein M, Katzman R, Price D, Stadlan EM: Clinical diagnosis of Alzheimer's disease: report of the NINCDS-ADRDA Work Group under the auspices of Department of Health and Human Services Task Force on Alzheimer's Disease. Neurology. 1984;34:939-944.
33. Paquet C, Mouton-Liger F, Meurs EF, Mazot P, Bouras C, Pradier L, Gray F, Hugon J: The PKR activator PACT is induced by Abeta: involvement in Alzheimer's disease. Brain Pathol. 2012;22:219-229.
34. Prange O, Wong TP, Gerrow K, Wang YT, El-Husseini A: A balance between excitatory and inhibitory synapses is controlled by PSD-95 and neuroligin. Proc Natl Acad Sci USA. 2004;101:13915-13920.
35. Schneider F, Baldauf K, Wetzel W, Reymann KG: Behavioral and EEG changes in male 5xFAD mice. Physiol Behav. 2014;135:25-33.
36. Girault JA, Costa A, Derkinderen P, Studler JM, Toutant M: FAK and PYK2/CAKbeta in the nervous system: a link between neuronal activity, plasticity and survival? Trends Neurosci. 1999;22:257-263.
37. Park SY, Avraham HK, Avraham S: RAFTK/Pyk2 activation is mediated by trans-acting autophosphorylation in a Src-independent manner. J Biol Chem. 2004;279:33315-33322.
38. Manders EMM, Verbeek FJ, Aten JA: Measurement of colocalization of objects in dual-color confocal images. J Microscopy 1992;169:375–382.
39. Grinan-Ferre C, Sarroca S, Ivanova A, Puigoriol-Illamola D, Aguado F, Camins A, Sanfeliu C, Pallas M: Epigenetic mechanisms underlying cognitive impairment and Alzheimer disease hallmarks in 5XFAD mice. Aging (Albany NY). 2016;8:664-684.
40. Hongpaisan J, Sun MK, Alkon DL: PKC epsilon activation prevents synaptic loss, Abeta elevation, and cognitive deficits in Alzheimer's disease transgenic mice. J Neurosci. 2011;31:630-643.
41. Shao CY, Mirra SS, Sait HB, Sacktor TC, Sigurdsson EM: Postsynaptic degeneration as revealed by PSD-95 reduction occurs after advanced Abeta and tau pathology in transgenic mouse models of Alzheimer's disease. Acta Neuropathol. 2011;122:285-292.
42. Hossain MI, Roulston CL, Kamaruddin MA, Chu PW, Ng DC, Dusting GJ, Bjorge JD, Williamson NA, Fujita DJ, Cheung SN, et al: A truncated fragment of Src protein kinase generated by calpain-mediated cleavage is a mediator of neuronal death in excitotoxicity. J Biol Chem. 2013;288:9696-9709.
43. Pozueta J, Lefort R, Shelanski ML: Synaptic changes in Alzheimer's disease and its models. Neuroscience. 2013;251:51-65.
44. Sheng M, Sabatini BL, Sudhof TC: Synapses and Alzheimer's disease. Cold Spring Harb Perspect Biol. 2012;4.
45. Tu S, Okamoto S, Lipton SA, Xu H: Oligomeric Abeta-induced synaptic dysfunction in Alzheimer's disease. Mol Neurodegener. 2014;9:48.
46. Lambert MP, Barlow AK, Chromy BA, Edwards C, Freed R, Liosatos M, Morgan TE, Rozovsky I, Trommer B, Viola KL, et al: Diffusible, nonfibrillar ligands derived from Abeta1-42 are potent central nervous system neurotoxins. Proc Natl Acad Sci U S A. 1998;95:6448-6453.

47. Pena F, Ordaz B, Balleza-Tapia H, Bernal-Pedraza R, Marquez-Ramos A, Carmona-Aparicio L, Giordano M: Beta-amyloid protein (25-35) disrupts hippocampal network activity: role of Fyn-kinase. Hippocampus. 2010;20:78-96.
48. Minami SS, Clifford TG, Hoe HS, Matsuoka Y, Rebeck GW: Fyn knock-down increases Abeta, decreases phospho-tau, and worsens spatial learning in 3xTg-AD mice. Neurobiol Aging. 2012;33:825 e815-824.
49. Kaufman AC, Salazar SV, Haas LT, Yang J, Kostylev MA, Jeng AT, Robinson SA, Gunther EC, van Dyck CH, Nygaard HB, Strittmatter SM: Fyn inhibition rescues established memory and synapse loss in Alzheimer mice. Ann Neurol. 2015;77:953-971.
50. Smith LM, Zhu R, Strittmatter SM: Disease-modifying benefit of Fyn blockade persists after washout in mouse Alzheimer's model. Neuropharmacology. 2018;130:54-61.
51. Li C, Gotz J: Somatodendritic accumulation of Tau in Alzheimer's disease is promoted by Fyn-mediated local protein translation. EMBO J. 2017;36:3120-3138.
52. Ittner LM, Ke YD, Delerue F, Bi M, Gladbach A, van Eersel J, Wolfing H, Chieng BC, Christie MJ, Napier IA, et al: Dendritic function of tau mediates amyloid-beta toxicity in Alzheimer's disease mouse models. Cell. 2010;142:387-397.
53. Dunning CJ, Black HL, Andrews KL, Davenport EC, Conboy M, Chawla S, Dowle AA, Ashford D, Thomas JR, Evans GJ: Multisite tyrosine phosphorylation of the N-terminus of Mint1/X11alpha by Src kinase regulates the trafficking of amyloid precursor protein. J Neurochem. 2016;137:518-527.
54. Gianni D, Zambrano N, Bimonte M, Minopoli G, Mercken L, Talamo F, Scaloni A, Russo T: Platelet-derived growth factor induces the beta-gamma-secretase-mediated cleavage of Alzheimer's amyloid precursor protein through a Src-Rac-dependent pathway. J Biol Chem. 2003;278:9290-9297.
55. Antonios G, Borgers H, Richard BC, Brauss A, Meissner J, Weggen S, Pena V, Pillot T, Davies SL, Bakrania P, et al: Alzheimer therapy with an antibody against N-terminal Abeta 4-X and pyroglutamate Abeta 3-X. Sci Rep. 2015;5:17338.
56. Bhattacharya S, Haertel C, Maelicke A, Montag D: Galantamine slows down plaque formation and behavioral decline in the 5XFAD mouse model of Alzheimer's disease. PLoS One. 2014;9:e89454.
57. MacPherson KP, Sompol P, Kannarkat GT, Chang J, Sniffen L, Wildner ME, Norris CM, Tansey MG: Peripheral administration of the soluble TNF inhibitor XPro1595 modifies brain immune cell profiles, decreases beta-amyloid plaque load, and rescues impaired long-term potentiation in 5xFAD mice. Neurobiol Dis. 2017;102:81-95.
58. Aytan N, Choi JK, Carreras I, Kowall NW, Jenkins BG, Dedeoglu A: Combination therapy in a transgenic model of Alzheimer's disease. Exp Neurol. 2013;250:228-238.
59. Castellani RJ, Lee HG, Siedlak SL, Nunomura A, Hayashi T, Nakamura M, Zhu X, Perry G, Smith MA: Reexamining Alzheimer's disease: evidence for a protective role for amyloid-beta protein precursor and amyloid-beta. J Alzheimers Dis. 2009;18:447-452.
60. Cohen E, Paulsson JF, Blinder P, Burstyn-Cohen T, Du D, Estepa G, Adame A, Pham HM, Holzenberger M, Kelly JW, et al: Reduced IGF-1 signaling delays age-associated proteotoxicity in mice. Cell. 2009;139:1157-1169.

Figure legends

Figure 1. Pyk2 in Alzheimer disease patients and 5XFAD mice. (**A**) Immunoblotting for Pyk2 and tubulin as a loading control, in human post-mortem prefrontal **cortex** (top panel) and **hippocampus** (bottom panel) samples from controls (**Cnt**) and **AD** patients. (**B**) Densitometric quantification of results as in (A) for prefrontal cortex, unpaired t-test $t_8 = 0.22$, ns (n = 5 per group), and hippocampus unpaired t-test $t_{32} = 0.76$, ns (n = 15 and 19 per group). (**C**) Immunoblotting for Pyk2, phosphoTyr402-Pyk2 (pY402-Pyk2) and tubulin as a loading control in 8-month (top panel) and 3-month (bottom panel) WT and 5XFAD mice. In A and C molecular weight markers position is indicated in kDa. (**D-E**) Densitometric quantification of results as in (C) for Pyk2 and pY402-Pyk2 in 8-month (**D**) and 3-month (**E**) old mice. In B, D, E, data were normalized to tubulin for each sample and expressed percentage of the mean of WT/controls and means and SEM are indicated. Unpaired t-test: (D) Pyk2, $t_{13} = 0.73$, ns; pY402-Pyk2, $t_{16} = 2.78$, $p = 0.013$ (n = 6 WT, 12 5XFAD), (E) Pyk2, $t_{13} = 0.17$, ns; pY402-Pyk2, $t_{12} = 0.24$, ns (n = 6-8 WT, 8 5XFAD).

Figure 2. Pyk2 is colocalized with Aβ in hippocampal neuropil of 5XFAD mice. (**A**) Stitched confocal images of Pyk2 and Aβ immunoreactivity in the hippocampus of 5XFAD mice. Scale bar 450 µm. (**B**) Higher magnification of Pyk2 and Aβ immunostaining in the rectangle in (A). Scale bar, 50 µm. (**C**) Optical density quantification of Pyk2 and Aβ staining in an Aβ-plaque indicated by a dashed line in (B). The intensity of the two immunoreactivities varies in an opposite manner. (**D**) High magnification of the area indicated (yellow box) in (B). From left to right, panels correspond to Pyk2, Aβ, double immunostaining, and colocalization index (Coloc, indicated in white). Scale bar, 5 µm. (**E**) Quantification of Pyk2 and Aβ colocalization using the Manders coefficient in 3 hippocampal regions, as in (I). Data are means ± SEM, n = 3 photos per mouse, 3 mice. (**F**) Pyk2/β-amyloid interaction revealed by *in situ* PLA in the hippocampus of 5XFAD mice. Control is provided by incubation with a **single antibody**, which did not generate specific signal, whereas with the **two antibodies** an amplification appears as red dots indicating a close proximity of the two proteins. Nuclei are stained in blue with DAPI. *Left panels*, low

magnification confocal images. Scale bar 50 µm. *Right panels*, higher magnification of Pyk2/β-amyloid interaction in boxed areas in the left panels. Scale bar 20 µm.

Figure 3. Behavioral phenotype of 5XFAD x Pyk2$^{-/-}$ mice. (**A**) Immunoblotting for Pyk2 and tubulin as a loading control in 8-month WT, Pyk2$^{-/-}$, 5XFAD, and 5XFAD x Pyk2$^{-/-}$ (double mutant, DM) mice. (**B**) Spontaneous locomotor activity in the open field of these mice monitored during 30 min (wt, n = 12, Pyk2-/-, n = 6, 5XFAD, n = 14, DM, n = 14). (**C-D**) Novel object recognition test. (**C**) **Short-term memory** was evaluated as the percentage of total time exploring the new object (object B) and old object (object A) 20 min after the training session. (**D**) **Long-term memory** was evaluated as the percentage of total time exploring the new object (object C) and old object (object B) 24 h after training. Statistical analysis, 1-way ANOVA, (C), $F_{(7, 86)}$ = 20.85, $p<10^{-4}$, (D) $F_{(7, 84)}$ = 3.69, p = 0.0016. Post-hoc Holm-Sidak's test within each genotype, ** p<0.01, **** $p<10^{-4}$. In (C-D), wt, n = 11, Pyk2$^{-/-}$, n = 11, 5XFAD, n = 13, DM, n = 12. (**E**) Passive avoidance test. The latency to step-through was measured before (**Training**) and 24 h after (**Testing**) receiving an electric shock. Two-way ANOVA: interaction, $F_{(3, 47)}$ = 6.83, p = 0.0007, time, $F_{(1, 47)}$ = 92.15, $p<10^{-4}$, genotype, $F_{(3, 47)}$ = 7.302, p = 0.0004, Holm-Sidak's test vs WT, **** $p<10^{-4}$. Wt, n = 11, Pyk2$^{-/-}$, n = 13, 5XFAD, n = 11, DM, n = 16. (**E**) Elevated plus-maze. The time spent in the open arms was monitored for 5 min. One-way ANOVA, $F_{(3, 43)}$ = 5.49, p = 0.003, Holm-Sidak's test vs WT, * p<0.05. Wt, n = 11, Pyk2$^{-/-}$, n = 8, 5XFAD, n = 13, DM, n = 15.

Figure 4. Histological phenotype of 5XFAD x Pyk2$^{-/-}$ mice. (**A**) Confocal image of PSD-95 immunofluorescence in CA1 *stratum radiatum* of 8-month WT, Pyk2$^{-/-}$, 5XFAD and 5XFAD x Pyk2$^{-/-}$ double mutant mice, as indicated. Scale bar 10 µm. (**B**) Quantification of the number of PSD-95-positive puncta per field as in (A), n = 7-9 mice per group. One-way ANOVA, $F_{(3, 29)}$ = 23.09, $p < 10^{-4}$, post-hoc Holm-Sidak's test, *** p<0.001. (**C**) Synaptophysin immunofluorescence, as in (A). Scale bar 5 µm. (**D**) Quantification of the number of synaptophysin-positive puncta per field as in (C),), n = 7-9 mice per group. One-way ANOVA, $F_{(3, 29)}$ = 10.92, $p < 10^{-4}$, post-hoc Holm-Sidak's test, *** p<0.001. (**E**) Aβ immunofluorescence in the hippocampus of 8-month 5XFAD and 5XFAD x Pyk2$^{-/-}$ mice. Scale bar 500 µm. (**F**)

Quantification of Aβ-positive plaques in CA1, CA3 and DG of 5XFAD and 5XFAD x Pyk2$^{-/-}$ mice. Genotype comparison for each region with Mann-Whitney test. ** $p<0.01$ (n = 3-6 mice per genotype). (**G**) Immunoblotting for GFAP and tubulin as a loading control in the hippocampus of the 4 genotypes. (**H**) Densitometric quantification of results as in (I). Data are means ± SEM. One-way ANOVA, $F_{(3, 18)} = 14.19$, $p<10^{-4}$, Holm-Sidak's test vs WT, ** $p<0.01$, *** $p<0.001$, n = 5-6 mice per group.

Figure 5. Pyk2 overexpression in the hippocampus of 5XFAD mice improves some behavioral alterations. (**A**) GFP fluorescence in the dorsal hippocampus of 8-month WT and 5XFAD mice bilaterally injected in the dorsal hippocampus, 3 weeks before, with AAV expressing GFP (WT/GFP and 5XFAD/GFP) or Pyk2 and GFP (5XFAD/Pyk2) under the control of CaMKIIα promoter (stitched pictures). Scale bar 500 µm. (**B**) Immunoblotting for Pyk2, phosphoTyr402-Pyk2 (pY402-Pyk2) and tubulin as a loading control in the 3 groups of mice. (**C-D**) Densitometric quantification of Pyk2 (**C**) and pY402-Pyk2 (**D**) as in (B). One-way ANOVA, Pyk2, $F_{(2, 22)} = 5.49$, $p = 0.012$, pY402-Pyk2, $F_{(2, 19)} = 7.91$, $p = 0.003$, n = 6-9 mice per group. (**E**) Elevated plus-maze. The time spent in the open arms was monitored for 5 min in WT/GFP (n = 13), 5XFAD-GFP (n = 9) and 5XFAD-Pyk2 (n = 12) mice. One-way ANOVA, $F_{(2, 31)} = 6.94$, $p = 0.003$. (**F**) Spontaneous locomotor activity in the open field monitored in all groups during 30 min (10-13 mice per group). (**G**) Passive avoidance test. The latency to step-through was measured before (**Training**) and 24 h after (**Testing**) receiving an electric shock (10-12 mice per group). Two-way ANOVA, interaction, $F_{(2, 29)} = 4.28$, $p = 0.02$, time, $F_{(1, 29)} = 42.9$, $p < 0.0001$, groups, $F_{(2, 29)} = 2.58$, $p = 0.09$. (**H-I**) Novel object recognition test. (**H**) **Short-term memory** was evaluated as the percentage of time exploring the new object (object B) and the old object (object A) 20 min after the training session. (**I**) **Long-term memory** was evaluated as the percentage of time exploring the new object (object C) and the old object (object B) 24 h after training (9-11 mice per group). Statistical analysis, 1-way ANOVA, (H), $F_{(5, 62)} = 31.5$, $p<10^{-4}$, (I), $F_{(5, 58)} = 23.2$, $p<10^{-4}$. In **C-E** and **G-I** post-hoc test was Holms-Sidak, * $p<0.05$, ** $p<0.01$, **** $p<10^{-4}$**.**

Figure 6. Neuropathology in 5XFAD mice overexpressing Pyk2 in the hippocampus. (**A**) Aβ immunofluorescence microscopy imaging in the dorsal hippocampus of 8-month WT and 5XFAD mice injected with AAV expressing GFP without or with Pyk2, as indicted, as in Fig. 3 (stitched pictures). Scale bar 500 µm. (**B**) Quantification of Aβ-positive plaques in CA1, CA3 and DG of 5XFAD/GFP and 5XFAD/Pyk2 mice (n = 8-11 mice per group). Unpaired t-test, CA1 t_{17} = 2.6, p = 0.02, CA3 t_{17} = 2.73, p = 0.014, DG t_{17} = 2.6, p = 0.02. (**C**) Immunoblotting for GFAP and tubulin as a loading control in the hippocampus of WT/GFP, 5XFAD/GFP and 5XFAD/Pyk2 mice. (**D**) Densitometric quantification of results as in (C). One-way ANOVA $F_{(2, 18)}$ = 28.8, $p<10^{-4}$. Holm-Sidak's test vs WT/GFP, **** $p<10^{-4}$. Data are means + SEM (6-9 mice per group). (**E**) Confocal image of PSD-95 immunofluorescence in CA1 *stratum radiatum* of 8-month WT or 5XFAD mice injected in the hippocampus with AAV expressing GFP without or with Pyk2, as indicted, as in Fig. 3. Scale bar 10 µm. (**F**) Quantification of the number of PSD-95-positive puncta per field as in (E), n = 4-8 mice per group. Kruskal-Wallis test, p = 0.025, post-hoc Dunn's test, * p<0.05. (**G**) Synaptophysin immunofluorescence, as in (E). Scale bar 5 µm. (**H**) Quantification of the number of synaptophysin-positive puncta per field as in (G), n = 4-8 mice per group. Kruskal-Wallis test, p = 0.036, post-hoc Dunn's test, * p<0.05.

Figure 7. Src alterations in hippocampus of Pyk2-/- and 5XFAD mice. (**A**) Immunoblotting for Src (antibody reacting with the C-terminus) and tubulin as a loading control in the hippocampus of $Pyk2^{+/+}$, $Pyk2^{+/-}$ and $Pyk2^{-/-}$ mice. The position of full-length (66 kDa) and cleaved (52 kDa) Src is indicated. (**B**) Densitometric quantification of results as in (A), n = 6-11 mice per group. One-way ANOVA 66-kDa Src $F_{(2, 25)}$ = 35.6, $p<10^{-4}$, 52-kDa Src $F_{(2, 25)}$ = 12.2, p = 0.0002, post-hoc Holm-Sidak's test vs $Pyk2^{+/+}$, * p<0.05, **** $p<10^{-4}$. (**C**) Immunoblotting for Src and tubulin in WT and 5XFAD mice. (**D**) Densitometric quantification of Src in WT (n = 12) and 5XFAD (n = 21) mice. 66-kDa-Src, t_{31} = 1.86, 52-kDa-Src, t_{31} = 2.21, * p<0.05. (**E**) Immunoblotting for Src and tubulin in $Pyk2^{-/-}$, 5XFAD and 5XFAD x $Pyk2^{-/-}$ double mutant mice, as indicated. (**F**) Densitometric quantification of results as in (E), n = 6-11 mice per group. One-way ANOVA 66-kDa Src, $F_{(3, 31)}$ = 1.89, ns, 52-kDa Src, $F_{(3, 31)}$ = 4.685, p = 0.008, post-hoc Holm-Sidak's test vs WT, * p<0.05, ** p<0.01. (**G**) Immunoblotting for Src and tubulin as a loading control in the hippocampus of WT/GFP, 5XFAD/GFP and 5XFAD/Pyk2 mice, as in Fig. 5. (**H**) Densitometric quantification of results as in (D), n = 6-15 mice per group. One-way

ANOVA 66-kDa Src, $F_{(2, 22)} = 0.89$, $p = 0.42$, 52-kDa Src, $F_{(2, 20)} = 7.6$, $p = 0.0035$. Holm-Sidak's test vs WT/GFP, * $p<0.05$. (B, C, E) data are means + SEM. (A, D) Molecular weight markers positions are indicated in kDa.

Highlights

- Pyk2 gene (PTK2B) was reported associated with risk for Alzheimer's disease
- Pyk2 protein levels were not altered in hippocampus of AD patients or mouse 5XFAD model
- Pyk2 autophosphorylation was decreased in hippocampus of 5XFAD mice
- Crossing Pyk2 KO and 5XFAD mice did not alter the severity of the disease
- Pyk2 overexpression improved behavioral and histological alterations in 5XFAD mice

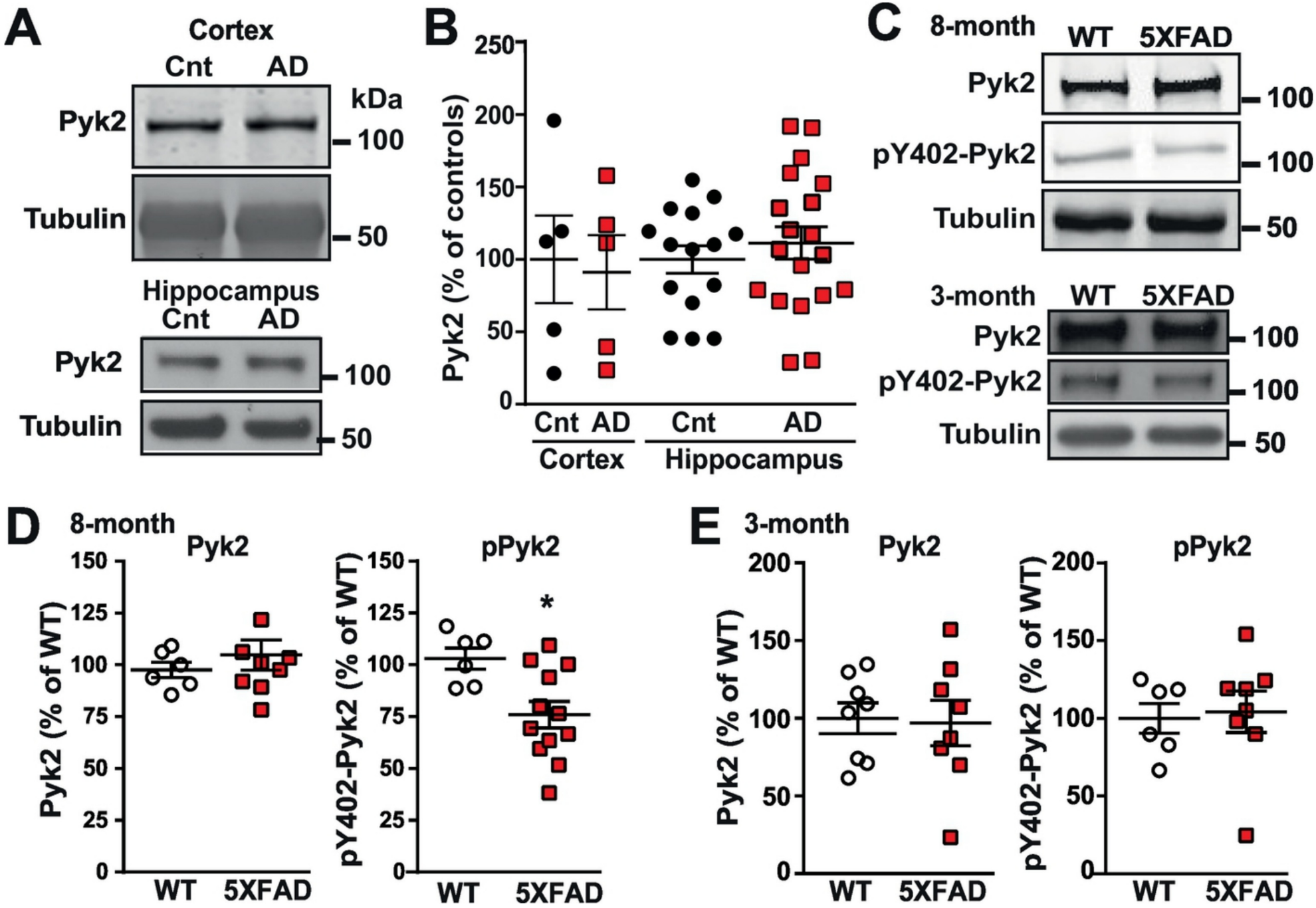
A
Cortex
Cnt
AD
kDa
Pyk2
100
Tubulin
50
Hippocampus
Cnt
AD
Pyk2
100
Tubulin
50
B
Pyk2 (% of controls)
250
200
150
100
50
0
Cnt
AD
Cnt
AD
Cortex
Hippocampus
C
8-month
WT
5XFAD
Pyk2
100
pY402-Pyk2
100
Tubulin
50
3-month
WT
5XFAD
Pyk2
100
pY402-Pyk2
100
Tubulin
50
D
8-month
Pyk2
Pyk2 (% of WT)
150
125
100
75
50
25
0
WT
5XFAD
pPyk2
pY402-Pyk2 (% of WT)
*
WT
5XFAD
E
3-month
Pyk2
Pyk2 (% of WT)
200
150
100
50
0
WT
5XFAD
pPyk2
pY402-Pyk2 (% of WT)
WT
5XFAD

Figure 1

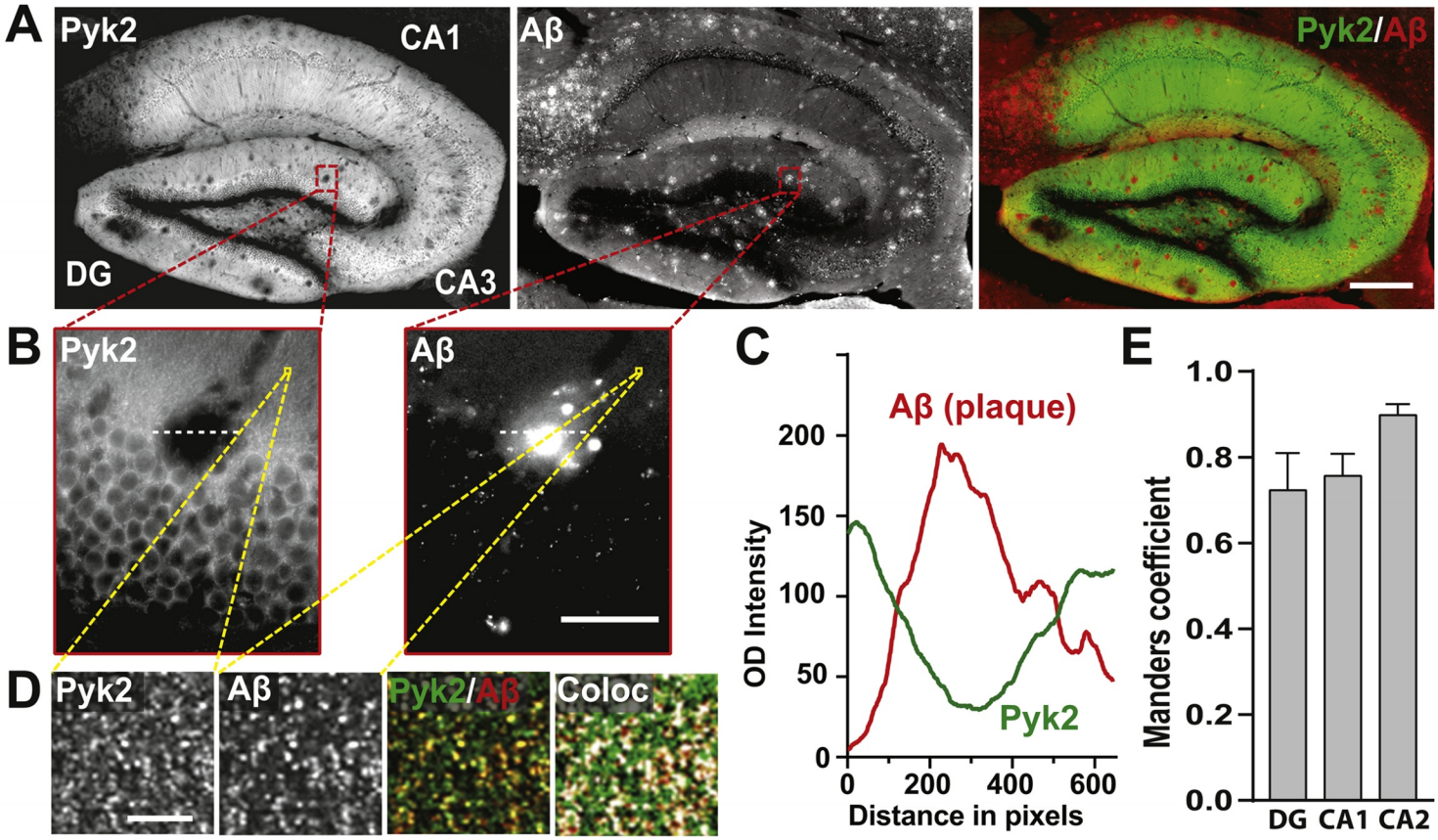
A
Pyk2
CA1
DG
CA3
Aβ
Pyk2/Aβ
B
Pyk2
Aβ
C
Aβ (plaque)
Pyk2
OD Intensity
Distance in pixels
E
Manders coefficient
DG CA1 CA2
D
Pyk2
Aβ
Pyk2/Aβ
Coloc

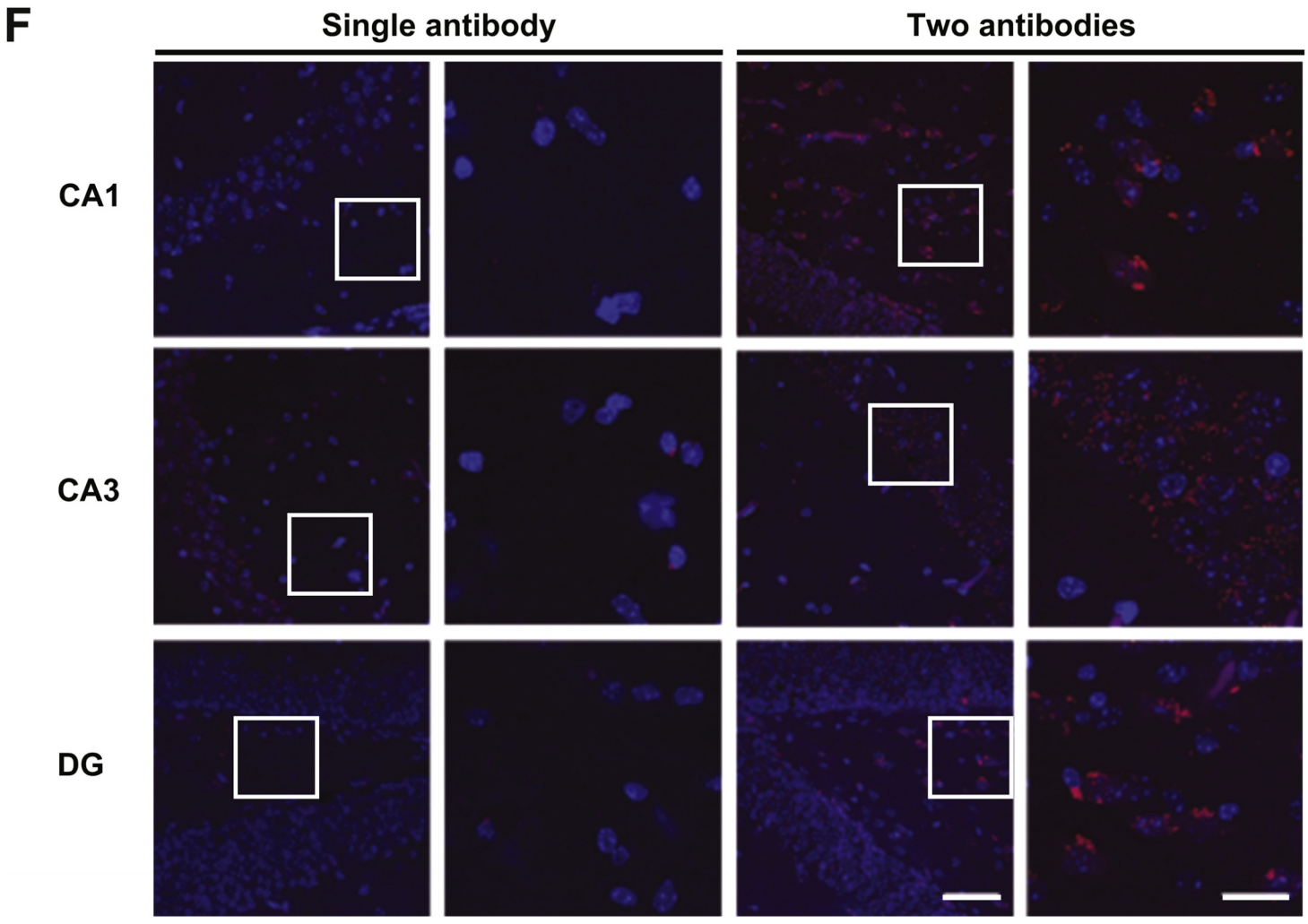
F
Single antibody
Two antibodies
CA1
CA3
DG

Figure 2

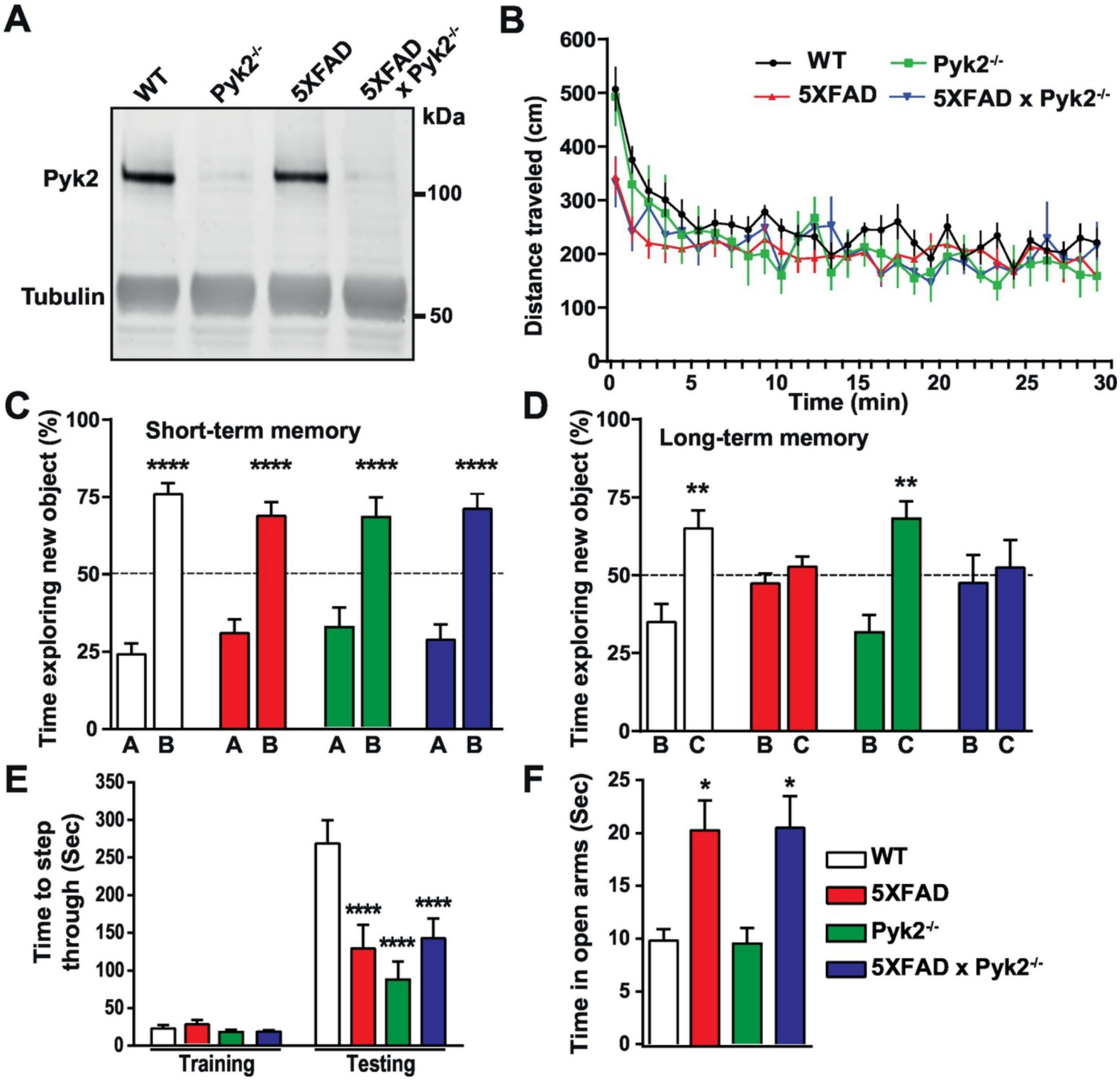
A
WT
Pyk2-/-
5XFAD
5XFAD x Pyk2-/-
kDa
Pyk2
Tubulin
100
50
B
WT
Pyk2-/-
5XFAD
5XFAD x Pyk2-/-
Distance traveled (cm)
Time (min)
C
Short-term memory
Time exploring new object (%)
****
A B
D
Long-term memory
Time exploring new object (%)
**
B C
E
Time to step through (Sec)
****
Training
Testing
F
Time in open arms (Sec)
*
WT
5XFAD
Pyk2-/-
5XFAD x Pyk2-/-

Figure 3

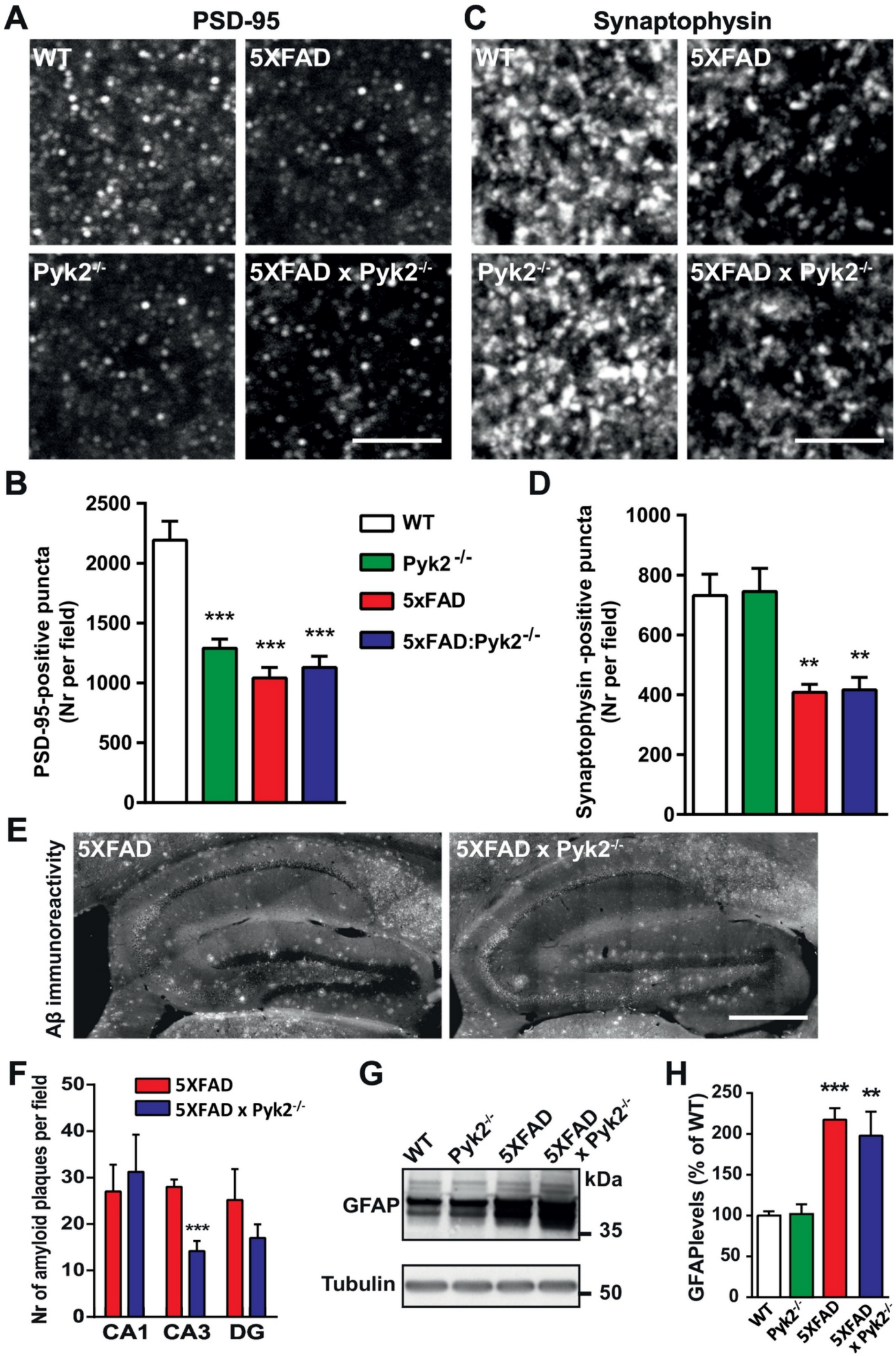
A
PSD-95
WT
5XFAD
Pyk2-/-
5XFAD x Pyk2-/-
C
Synaptophysin
WT
5XFAD
Pyk2-/-
5XFAD x Pyk2-/-
B
PSD-95-positive puncta (Nr per field)
2500
2000
1500
1000
500
0
***
***
***
WT
Pyk2 -/-
5xFAD
5xFAD:Pyk2-/-
D
Synaptophysin -positive puncta (Nr per field)
1000
800
600
400
200
0
**
**
E
Aβ immunoreactivity
5XFAD
5XFAD x Pyk2-/-
F
Nr of amyloid plaques per field
50
40
30
20
10
0
5XFAD
5XFAD x Pyk2-/-
***
CA1
CA3
DG
G
WT
Pyk2-/-
5XFAD
5XFAD x Pyk2-/-
kDa
GFAP
35
Tubulin
50
H
GFAPlevels (% of WT)
250
200
150
100
50
0
***
**
WT
Pyk2-/-
5XFAD
5XFAD x Pyk2-/-

Figure 4

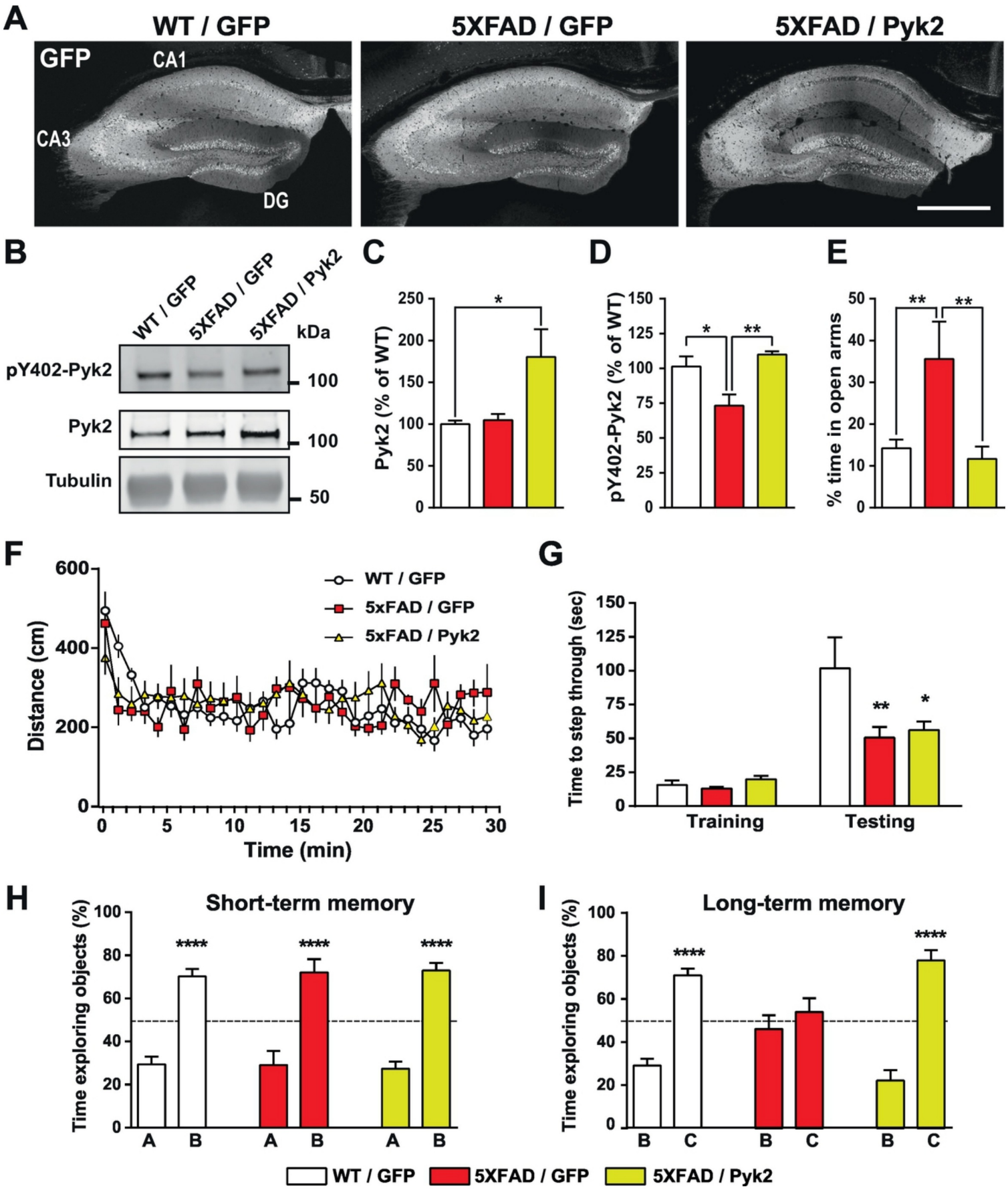
A
WT / GFP
5XFAD / GFP
5XFAD / Pyk2
GFP
CA1
CA3
DG
B
WT / GFP
5XFAD / GFP
5XFAD / Pyk2
kDa
pY402-Pyk2
100
Pyk2
100
Tubulin
50
C
Pyk2 (% of WT)
D
pY402-Pyk2 (% of WT)
E
% time in open arms
F
WT / GFP
5xFAD / GFP
5xFAD / Pyk2
Distance (cm)
Time (min)
G
Time to step through (sec)
Training
Testing
H
Short-term memory
Time exploring objects (%)
A
B
I
Long-term memory
Time exploring objects (%)
B
C
WT / GFP
5XFAD / GFP
5XFAD / Pyk2

Figure 5

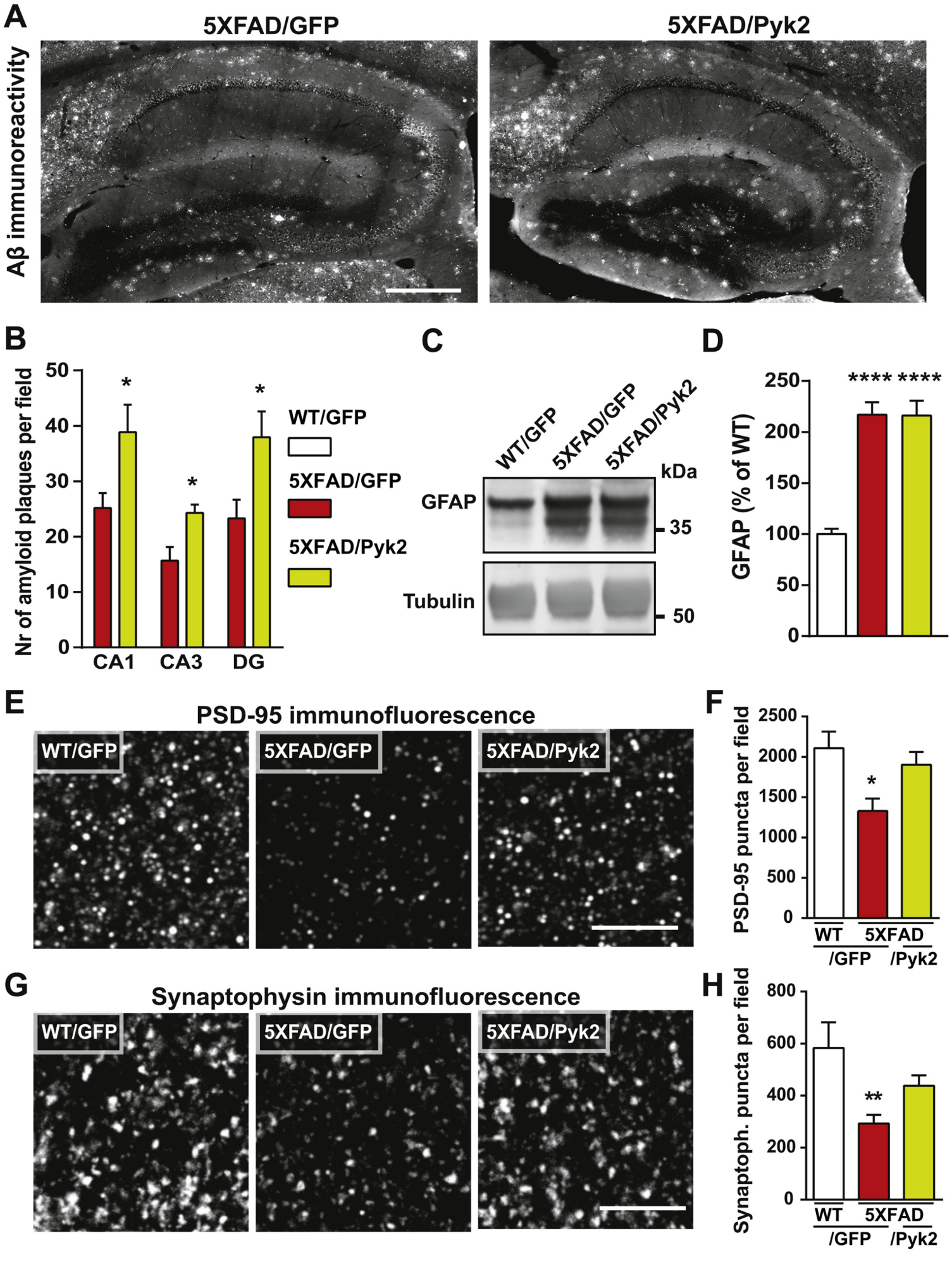
A
5XFAD/GFP
5XFAD/Pyk2
Aβ immunoreactivity
B
Nr of amyloid plaques per field
50
40
30
20
10
0
CA1
CA3
DG
WT/GFP
5XFAD/GFP
5XFAD/Pyk2
C
WT/GFP
5XFAD/GFP
5XFAD/Pyk2
kDa
GFAP
35
Tubulin
50
D
GFAP (% of WT)
250
200
150
100
50
0
**** ****
E
PSD-95 immunofluorescence
WT/GFP
5XFAD/GFP
5XFAD/Pyk2
F
PSD-95 puncta per field
2500
2000
1500
1000
500
0
WT /GFP
5XFAD /Pyk2
G
Synaptophysin immunofluorescence
WT/GFP
5XFAD/GFP
5XFAD/Pyk2
H
Synaptoph. puncta per field
800
600
400
200
0
WT /GFP
5XFAD /Pyk2

Figure 6

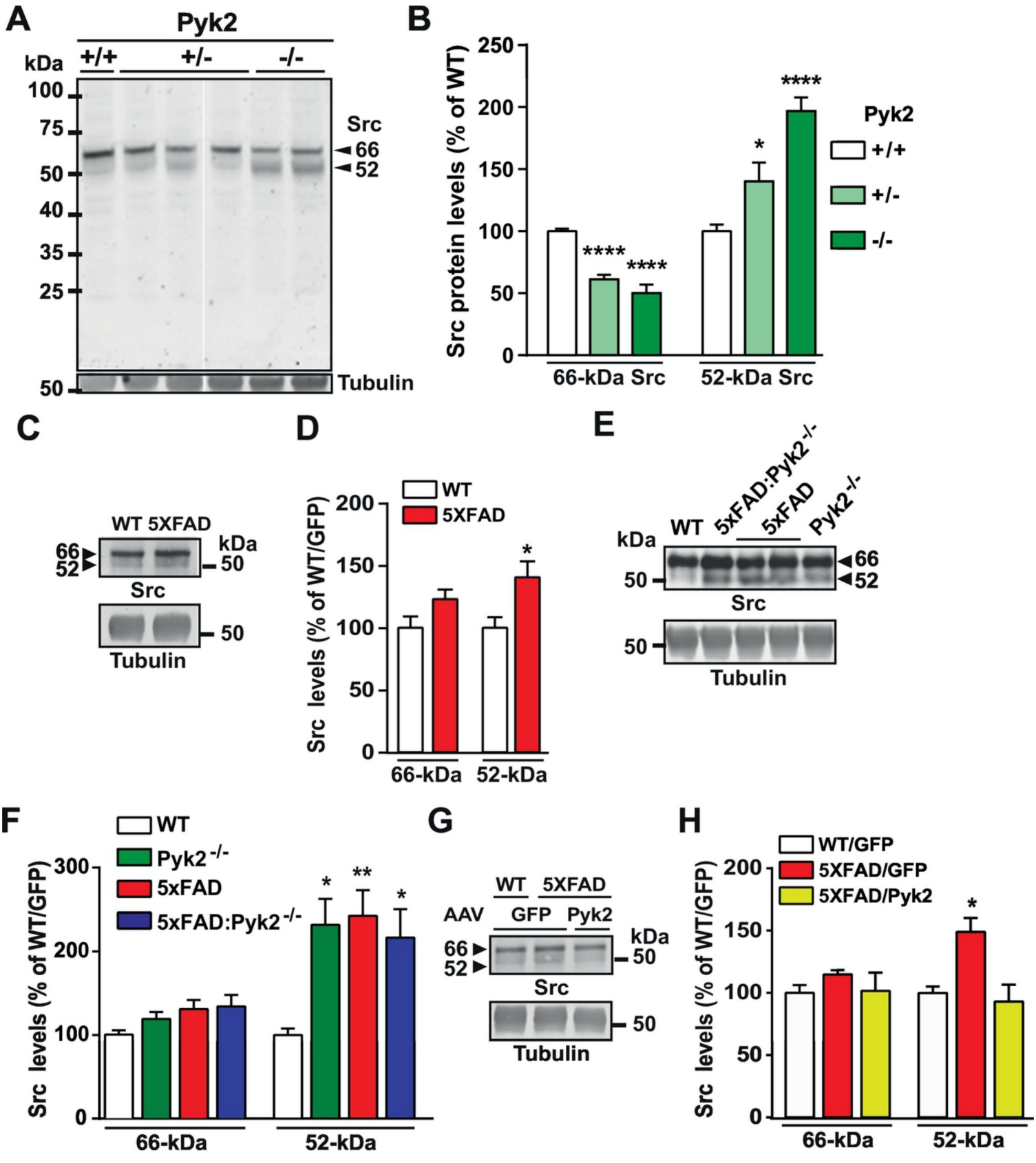
A
Pyk2
kDa
+/+
+/-
-/-
100
75
50
40
35
25
Src
66
52
50
Tubulin
B
Src protein levels (% of WT)
250
200
150
100
50
0
****
****
*
****
Pyk2
+/+
+/-
-/-
66-kDa Src
52-kDa Src
C
WT 5XFAD
66
52
kDa
50
Src
50
Tubulin
D
WT
5XFAD
Src levels (% of WT/GFP)
200
150
100
50
0
*
66-kDa
52-kDa
E
kDa
WT
5xFAD:Pyk2-/-
5xFAD
Pyk2-/-
50
66
52
Src
50
Tubulin
F
WT
Pyk2-/-
5xFAD
5xFAD:Pyk2-/-
Src levels (% of WT/GFP)
300
200
100
0
*
**
*
66-kDa
52-kDa
G
WT
5XFAD
AAV
GFP
Pyk2
kDa
66
52
50
Src
50
Tubulin
H
WT/GFP
5XFAD/GFP
5XFAD/Pyk2
Src levels (% of WT/GFP)
200
150
100
50
0
*
66-kDa
52-kDa

Figure 7